

APPLICATION OF NEAR INFRARED SPECTROSCOPY TO PULP
YIELD AND KAPPA NUMBER ESTIMATION

Except where reference is made to the work of others, the work described in this thesis is my own or was done in collaboration with my advisory committee. This thesis does not include proprietary or classified information.

Roy William Lightle Jr.

Certificate of Approval:

Steve R. Duke
Associate Professor
Chemical Engineering

Gopal A. Krishnagopalan, Chair
Professor
Chemical Engineering

Harry T. Cullinan
Professor
Chemical Engineering

Stephen L. McFarland
Acting Dean
Graduate School

APPLICATION OF NEAR INFRARED SPECTROSCOPY TO PULP
YIELD AND KAPPA NUMBER ESTIMATION

Roy William Lightle Jr.

A Thesis

Submitted to

the Graduate Faculty of

Auburn University

in Partial Fulfillment of the

Requirements for the

Degree of

Master of Science

Auburn, Alabama
August 7, 2006

APPLICATION OF NEAR INFRARED SPECTROSCOPY TO PULP
YIELD AND KAPPA NUMBER ESTIMATION

Roy William Lightle Jr.

Permission is granted to Auburn University to make copies of this thesis at its discretion, upon the request of individuals or institutions and at their expense. The author reserves all publication rights.

Signature of Author

Date of Graduation

VITA

Roy William Lightle Jr., son of Roy William Sr. and Deborah Kay Wolford Lightle, was born August 14, 1981 in New Orleans, Louisiana. He graduated from Perrysburg High School in 1999. He enrolled in Bowling Green State University in 1999 and later transferred to Auburn University in 2000. He interned for the Kimberly-Clark Corporation in 2001, gaining valuable experience in a corporate environment. He graduated from Auburn University with a Bachelor of Science in Chemical Engineering in August 2003. He entered Graduate School at Auburn University in the Department of Chemical Engineering in August 2003.

THESIS ABSTRACT

APPLICATION OF NEAR INFRARED SPECTROSCOPY TO PULP YIELD AND KAPPA NUMBER ESTIMATION

Roy William Lightle Jr.

Master of Science, August 7, 2006
(B.S.C.H.E. Auburn University, 2003)

114 Typed Pages

Directed by Gopal A. Krishnagopalan

This thesis presents an investigation into near infrared (NIR) spectroscopy as a technique for determining pulp yield and kappa number for kraft pulp and black liquor samples. It is believed that proper spectra collection and preprocessing techniques combined with a linear regression analysis can produce models that accurately predict pulp yield and kappa number. Currently, no instrument exists for estimating these values simultaneously. Methods for estimating yield and kappa number consist of lengthy lab based wet chemistry techniques. NIR reflectance spectroscopy has the potential of providing a single, relatively simple instrument solution for both of these measurements. NIR transmission spectroscopy of the black liquor may provide further information and process control capability. The ability to predict yield and kappa number is a valuable process control technology for use in kraft mills.

Samples of pulp with yield and kappa number ranges typical of mills were generated from the batch kraft digestion of softwood chips and liquor of varying EA. NIR spectra of the samples were collected using little or no sample pretreatment. The idea was to analyze the samples under conditions similar to a non-idealized mill environment. Different prototype NIR spectrometers were used covering a major portion of the NIR spectrum. Correlations between the pulp yield, kappa number, NIR reflectance data of the pulp and NIR transmission data of the black liquor have been developed. These lab based calibrations were used to predict kappa number and yield values for lab generated pulp samples. The calibration models were also able to accurately predict kappa values for unknown mill pulp samples.

ACKNOWLEDGEMENTS

The author would like to thank Dr. Gopal Krishnagopalan for his support, knowledge, motivation, and immense patience during the course of this research.

The author would like to thank Dr. Russell Hodges for the opportunity to be involved in a multi-disciplinary and very unique graduate research project. His assistance and knowledge were invaluable.

The author would like to thank Dr. Phillip Woodrow for his assistance, knowledge, and conversation.

The aforementioned were all instrumental in the development and success of this research.

Finally, the author would like to thank his parents for all the support, both emotive and fiscal.

Style manual or journal used Tappi Journal.

Computer software used Microsoft Office 2003, Matlab 7.0.

TABLE OF CONTENTS

LIST OF FIGURES.....	xi
INTRODUCTION.....	1
Significance of the Research.....	1
Objective and Scope.....	3
Wood Composition.....	4
Macrostructure.....	4
Microstructure.....	5
Molecular Level.....	6
Kraft Process.....	8
Process Nomenclature.....	8
Process Description.....	9
Prior Research.....	15
BACKGROUND.....	19
Spectroscopy.....	19
Spectra Linearization.....	25
Regression Techniques.....	27
Multiple Linear Regression.....	27
Principle Component Regression.....	28
Partial Least Squares Regression.....	28

Spectra Processing.....	29
Differentiation.....	29
Filtering.....	30
Signal Correction.....	30
EXPERIMENTAL METHODS.....	32
Overview.....	32
NIR Spectroscopy.....	33
Sample Preparation.....	34
NIR Analysis.....	38
Software.....	46
RESULTS AND DISCUSSION.....	48
Overview.....	48
Characteristic Spectra.....	49
Spectra Smoothing and Differentiation.....	55
Signal Correction.....	67
Pulp Calibration Models and Predictions.....	76
Black Liquor Calibration Models and Predictions.....	85
CONCLUSIONS.....	91
BIBLIOGRAPHY.....	93
APPENDIX A.....	95
APPENDIX B.....	99

LIST OF FIGURES

Figure 1: Key components of the kraft process.....	12
Figure 2: Block diagram of the kraft process.....	13
Figure 3: Chemical recovery cycle of the kraft process.....	14
Figure 4: The electromagnetic spectrum.....	22
Figure 5: Variables for use with the Beer-Lambert relation in transmission.....	23
Figure 6: Variables for use with the Beer-Lambert relation in reflectance.....	23
Figure 7: Typical optical spectrometer configuration.....	24
Figure 8: Bombs used during the cooking process.....	37
Figure 9: Data collection system.....	38
Figure 10: NIR transmission set-up.....	39
Figure 11: Hand press for sample preparation.....	40
Figure 12: Reflectance set-up.....	41
Figure 13: Rosemount AOTF-NIR system.....	41
Figure 14: Reflectance set-up.....	43
Figure 15: Prototype spectrometer.....	43
Figure 16: Picture of prototype spectrometer.....	45
Figure 17: Picture of reflectance set-up.....	45
Figure 18: Spectra collected using different light sources.....	51
Figure 19: Spectra of pulp from the Rosemount AOTF-NIR spectrometer.....	52

Figure 20: Spectra of pulp from the SWNIR prototype analyzer.....	53
Figure 21: Spectra of pulp from the LWNIR prototype analyzer.....	54
Figure 22: Oscillations in spectra caused by motor noise in the LWNIR analyzer.....	57
Figure 23: Close-up of unfiltered spectra from the LWNIR analyzer.....	58
Figure 24: Spectra from the LWNIR analyzer with some DCT filtering.....	59
Figure 25: Spectra form the LWNIR analyzer with considerable DCT filtering.....	60
Figure 26: First derivative of raw spectrum for the LWNIR analyzer.....	61
Figure 27: DCT filtered and differentiated spectrum from the LWNIR analyzer.....	62
Figure 28: Savitsky-Golay treated spectrum from the LWNIR analyzer.....	63
Figure 29: Savitsky-Golay treated spectra from the AOTF-NIR analyzer.....	64
Figure 30: Savitsky-Golay treated spectra from the SWNIR analyzer.....	65
Figure 31: Savitsky-Golay treated spectra from the LWNIR analyzer.....	66
Figure 32: DCT filtered spectra of one samples.....	69
Figure 33: Figure 32 spectra with SNV applied.....	70
Figure 34: Figure 32 spectra with MSC applied.....	71
Figure 35: Savitsky-Golay treated spectra from the LWNIR analyzer.....	72
Figure 36: Previous spectra with OSC applied.....	73
Figure 37: Three samples with widely varying kappa number.....	74
Figure 38: Previous spectra with OSC applied.....	75
Figure 39: Calibration curves for kappa measurement.....	78
Figure 40: Calibration curves for yield measurement.....	79
Figure 41: Prediction curve for kappa measurement.....	80
Figure 42: Prediction curve for yield measurement.....	81

Figure 43: Calibration curve for kappa measurement of mill samples.....	82
Figure 44: Prediction curve for kappa measurement of mill samples.....	83
Figure 45: Table of actual and predicted values for mill samples.....	84
Figure 46: Typical spectra for spent black liquor.....	86
Figure 47: Black liquor calibration curve for kappa measurement.....	87
Figure 48: Black liquor calibration curve for yield measurement.....	88
Figure 49: Black liquor prediction curve for kappa measurement.....	89
Figure 50: Black liquor prediction curve for yield measurement.....	90

INTRODUCTION

Significance of the Research

The focus of this research was the development of techniques and practices to implement near infrared (NIR) spectroscopy for the measurement of process variables important to the pulp and paper industry. The main focus was to utilize NIR spectroscopy for the determination of pulp yield and kappa number. This research will lead to the development of lab based and online analyzers capable of measuring pulp yield and kappa number. To achieve this analysis, proper mathematical models and spectral techniques must be developed and employed.

In the pulping process accurate analysis of pulp yield and quality is of considerable value. Pulp yield is an essential parameter having both economic as well as process importance. Knowledge of both yield and kappa number allows for control over pulp properties and more consistent pulp and paper products. The usefulness of these parameters warrants a robust technique for their determination.

In practice, yield determinations are generally inaccurate and are mostly estimated using production and inventory. The tests for kappa number are usually performed in a lab on a routine basis as a quality control test. Kappa tests are either performed by

manual titration or with the use of an automated titration system. The automated system is likely more accurate, but either procedure requires human input and may lead to variability in measurements. The results of the kappa measurements are generally used to determine the control action needed to keep the pulp quality within the specification. The infrequency of these tests gives poor approximations of actual values due to the variability and large amount of raw materials used in the pulping process. Furthermore, these tests cannot be used as an online real time process control tool.

There is clearly a need for a more accurate method of determining pulp yield and kappa number. NIR spectroscopy is a fast and relatively simple method for performing compositional analysis of pulp. The development of lab based and online NIR spectroscopy instruments for kappa and yield measurements will allow for unprecedented control in the kraft process.

Objective and Scope

The objective of this work was to develop techniques necessary to calibrate NIR spectroscopic equipment to estimate pulp yield and kappa number of kraft pulp. NIR measurements of the pulp itself and spent black liquor were investigated. Prototype optics benches designed by a third party company were used for the spectral analysis. The sample preparation and spectral methods used in this research are not the most robust lab based techniques available, but reflect a system that can be implemented online in a non-idealized mill environment. Such an environment requires simple durable instrumentation and minimal or no sample preparation. The specific objectives and approaches are stated below:

- Review and repeat previous research using the third party company's optics bench for NIR measurements.
- Determine the minimal amount of sample preparation necessary that allows for the collection of a useable spectrum.
- Determine the best arrangement for spectroscopic measurements of the pulp sample.
- Determine the best preprocessing and regression strategies for the development of pulp yield and kappa number calibration models.
- Investigate the ability to estimate yield and kappa number of both pulp and spent black liquor using spectroscopic measurements from the optics bench designed by the third party company.

Wood Composition

Wood is the most utilized resource for the production of cellulose containing products. Wood has many components to its structure which must be considered for its use in pulping. These components are considered as either being part of the woods macrostructure or microstructure. Further detail about the wood can be seen at the molecular level as well. Wood is classified as either hardwood (angiosperm) or softwood (gymnosperm). Both types of wood have the same components in their macrostructure and molecular level, but differ in their microstructure.

Macrostructure

It is easy to visualize all of the macrostructural components of wood considering a cross-sectional view of a tree trunk. On the outside of a tree is the outer bark which is made up of dead cells that provide physical and biological protection. The first interior layer of the wood is the inner bark or phloem. The phloem is a narrow layer of tissue that serves to conduct the sap or nutrients up and down the tree stem. Just inside the phloem is the cambium where new growth takes place.

The rate of growth in the cambium varies with season. Tree growth is accomplished through the deposition of successive layers of new cells on already existing fibers. Earlywood growth occurring in the spring and summer is characterized by thin wall fiber cells and latewood growth occurring in the fall is characterized by thick wall fiber cells. Trees are generally dormant in the winter months. This annual growth cycle with earlywood followed by latewood results in the annual ring pattern found in wood.

The trunk of the tree, not including the bark, is referred to as the xylem and contains the sapwood and heartwood. The sapwood is physiologically active (parenchyma cells only) and provides structural support, food storage and water conduction for the tree. The heartwood resides inside the sapwood and is made up of dead wood cells that provide only structural support. Inside the heartwood is juvenile wood made up of short fibers with low density. The juvenile wood surrounds the pith or center of the tree. The pith is composed entirely of parenchyma cells much like the sapwood. The last component of the wood macrostructure is the wood rays which are positioned radially and provide storage and lateral food movement from the phloem to the cambium and sapwood.

Microstructure

Considering the microstructure of wood, differences between hardwoods and softwoods are apparent. Hardwoods are more complex containing libriform fibers, vessel elements, fiber tracheids, ray cells, and parenchyma. Whereas softwoods only contain fiber tracheids, ray cells, and resin ducts. The relatively long and narrow libriform fibers of hardwoods function as support and the shorter and wider vessel elements aid in conducting water and nutrients. Ray cells in both hardwood and softwood and parenchyma in hardwood provide storage and conduction of water and nutrients. Resin ducts in softwoods secrete resins and prevent invasion of insects and pathogenic organisms. The tracheids are the individual fibers that make up most of the vertical structure of the wood. Softwood fibers are generally about twice as long as hardwood fibers. The greatest difference in hardwood and soft wood pertains to the weight and

volume percentages of various components like fibers, vessels, and parenchyma in the wood.

The wood fibers in hardwoods and softwoods can be broken down into additional components. A typical tracheid is composed of several layers. The middle lamella has a very high lignin content and separates two adjacent tracheids. The middle lamella is essentially what holds the fibers together. The tracheids each have a primary wall and secondary wall which contain microfibrils. Microfibrils are bundles of cellulose fibers and their orientation affects characteristics of pulp fibers. The primary wall is a mixture of hemicelluloses with random microfibril orientation. The three-layered secondary wall is located inside the primary wall and contains microfibrils with a specific orientation.

Molecular Level

At the molecular level hardwoods and softwoods contain the same components which are cellulose, hemicelluloses, lignin, and extractives. Hardwoods typically have higher concentrations of cellulose, hemicelluloses, and extractives, while softwood has a higher concentration of lignin.

Cellulose is a carbohydrate or more specifically a polysaccharide composed of repeating cellobiose molecules. Cellobiose is composed of two d-glucose molecules connected by a 1,4'- β -glycosidic bond. The size of cellulose molecules is quantified by their degree of polymerization (D.P.) which is the number of glucose units. Typically the D.P. is in the range of 600-1500 for most papermaking fibers. While cellulose exists in crystalline and amorphous states the high linearity of the cellulose molecule lends itself to a crystalline structure. This crystalline structure produces fibers which are difficult to

penetrate by solvents or reagents making them ideal for papermaking. Other properties of cellulosic fibers include high tensile strength, suppleness, resistance to plastic deformation, water insoluble, hydrophilic, wide range of dimensions, inherent bonding ability, ability to absorb modifying additives, chemically stable, and relatively colorless (1).

Hemicelluloses, on the other hand, are polymers made up of five different sugars; glucose, mannose, galactose, xylose, and arabinose. Glucose, mannose, and galactose are six carbon sugars whereas xylose and arabinose are five carbon sugars. Hemicelluloses generally exist in an amorphous state due to their inherent heterogeneous structure. This aspect makes hemicelluloses much more susceptible to solvation and degradation than cellulose. For this reason there is generally fair less hemicelluloses in pulp than in the original wood.

Lignin is an amorphous, highly polymerized substance that forms the middle lamella and serves as the cement that holds various fibers together. Lignin is obviously important for the structural integrity of the tree, but from a papermaking point of view is an undesirable constituent. The structure of lignin consists of phenyl propane units linked three dimensionally. In chemical pulping the linkage between the propane side and the benzene ring is broken in order to free the cellulosic fibers.

Extractives make up about 5% of wood and are a diverse class of wood components that are soluble in organic solvents. Extractives include; terpenoid compounds, resin acids, fatty acids, and alcohols. The compounds are generally recovered in the pulping process and sold as by-products.

Kraft Process

Process Nomenclature

White Liquor: A mixture of reacting and inactive chemicals dissolved in water and used for the cooking of wood chips to free cellulose fibers. The active chemicals are sodium hydroxide (NaOH) and sodium sulfide (Na₂S) and the dead load chemicals include sodium carbonate (Na₂CO₃), sodium sulfite (Na₂SO₃), sodium sulfate (Na₂SO₄), sodium thiosulfate (Na₂S₂O₃), sodium chloride (NaCl), and potassium chloride (KCl).

Black Liquor: A mixture of unreacted and dead load chemicals from the white liquor, along with lignin and some dissolved carbohydrates. This is the spent liquor from the cooking of wood chips.

Green Liquor: This is the dissolved smelt of sodium carbonate and sodium sulfide resulting from the burning of black liquor in a recovery furnace.

Effective Alkali (EA): This is the total sodium hydroxide in liquor at any given time. Sodium sulfide hydrolyses to produce sodium hydroxide. Thus the EA is the sum of the actual sodium hydroxide along with the sodium hydroxide formed from the hydrolysis of sodium sulfide.

As Na₂O: This a convention used to put all sodium salts in the liquor on a common basis for measurement. The sodium salts are expressed in Na₂O equivalents, referred to as grams or pounds of Na₂O per unit volume.

Process Description

In order to produce pulp for the manufacture of paper products or any cellulose containing product, the fibers that compose wood must be freed from their inherent structure. Pulping of wood is performed either by mechanical or chemical means. The idea in chemical pulping is to remove lignin, the amorphous polymer that holds the wood fibers together. Essentially, the wood is delignified and as a result the wood fibers are liberated.

The most common method used for wood pulping is the kraft process. Figure 1 and figure 2 show the key components and a block diagram of the kraft process, respectively. In the kraft process, wood chips and white liquor are added to a digester and cooked at a range of temperatures and times depending on the type of digester used. The amount of liquor charged in the reactor is determined from the bone dry weight of the wood and desired liquor to wood ratio.

The two types of digesters employed in the kraft process are either batch or continuous. Batch digesters are much like a pressure vessel while continuous digesters behave more like a plug-flow reactor. With a batch digester chips and white liquor are added to the vessel and the temperature is ramped up and the chips are cooked at a range from 155°C to 175°C for 1 to 3 hours. The continuous digester uses multiple zones which mimics in spatial coordinates the process that occurs in a batch digester based on time coordinates (2). Chips and white liquor are usually first combined in an impregnation vessel allowing the chemicals to begin to diffuse into the chips. The chips are then pumped into the impregnation zone in the top of the digester and then through an upper and lower heating zone to ramp up to the desired cooking temperature. The chips then go

to the cooking zone where most of the delignification occurs. Finally, the chips are partially washed in the washing zone and then blown apart by a pressure differential in the blow tank to release the liberated fibers from the chips.

After leaving the blow tank the pulp is sent to series of vacuum washers that serve to further remove the remaining organic and inorganic compounds remaining with the pulp fibers. The washer effluent is weak black liquor that can be used as make-up to the cooking process or in the washing zone of the continuous digester. Once the pulp is washed it is either sent to paper machines or a bleaching plant for the production of higher grade pulps.

The spent black liquor from the digester enters into a chemical recovery cycle. Figure 3 shows the chemical cycles of the process. The black liquor is first concentrated in a series of evaporators and then burned in a recovery furnace. In the furnace the organic compounds are oxidized and the inorganic chemicals remain and form a mixture referred to as smelt which contains sodium carbonate and sodium sulfide. The smelt and weak white liquor are combined in a dissolving tank and then sent to the green liquor clarifier. Suspended solids referred to as dregs settle out in the clarifier and are washed to remove additional useful inorganic chemicals before being sent to the landfill. The resulting green liquor from the clarifier is sent to storage tanks and eventually to a causticizing plant.

The causticizing plant serves to convert the green liquor into white liquor to eventually be used in the cooking process. Calcium oxide (CaO) in the form of lime is first added to the green liquor at the slaker. The calcium oxide and water react violently disintegrating the lime and allowing for the filtration of unwanted and inert materials

from the useful lime. The material that is filtered out is referred to as grits and is sent to the landfill. The remaining lime from the slaker is sent to the causticizer to complete the causticizing reaction. The slurry from the causticizer contains sodium hydroxide and lime mud (solid CaCO_3). The lime mud is removed from the slurry at the white liquor clarifiers and the resulting white liquor can once again be used at the digester. Lime and weak white liquor are recovered from the lime mud for reuse in the causticizing process.

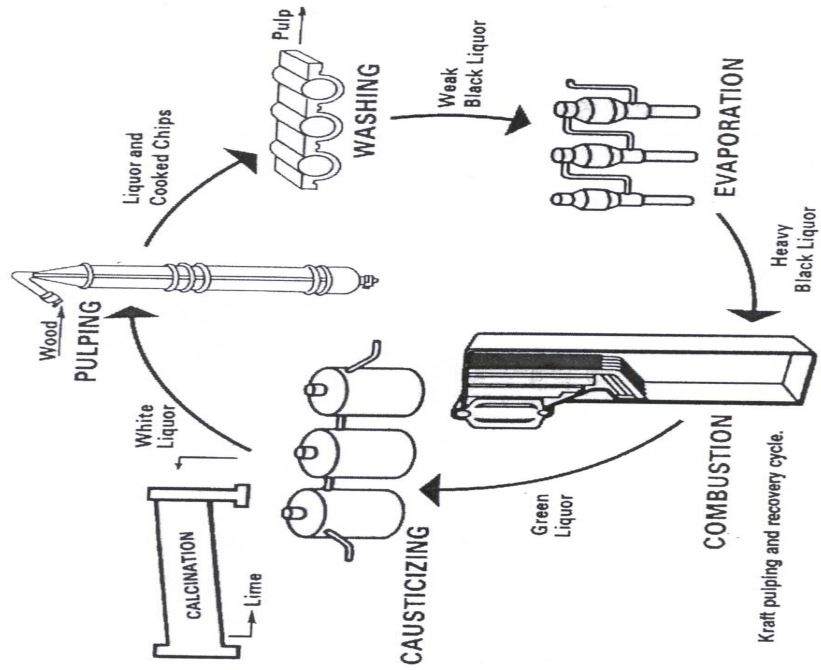


Figure 1: Key components of the kraft process (1).

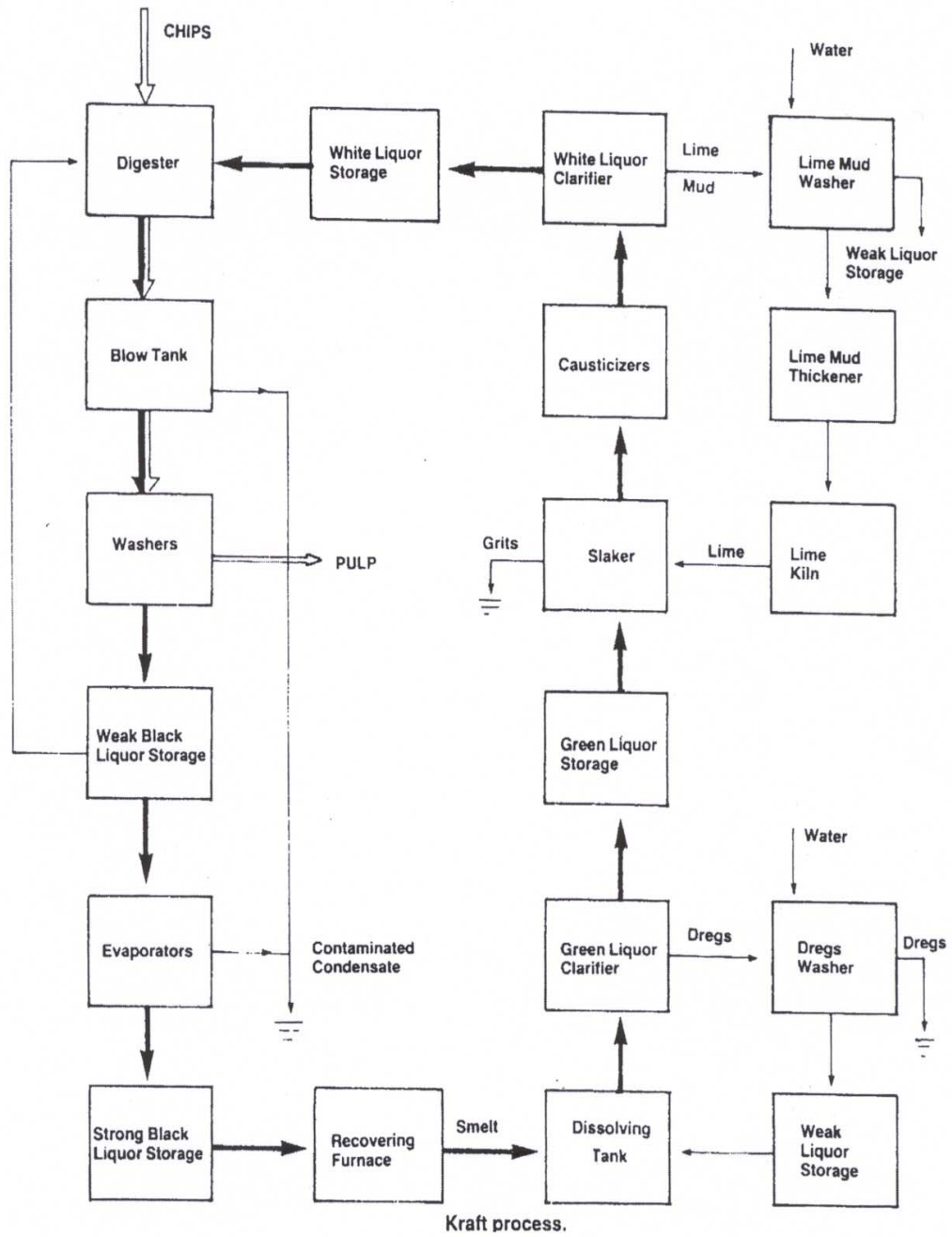


Figure 2: Block diagram of the kraft process (1).

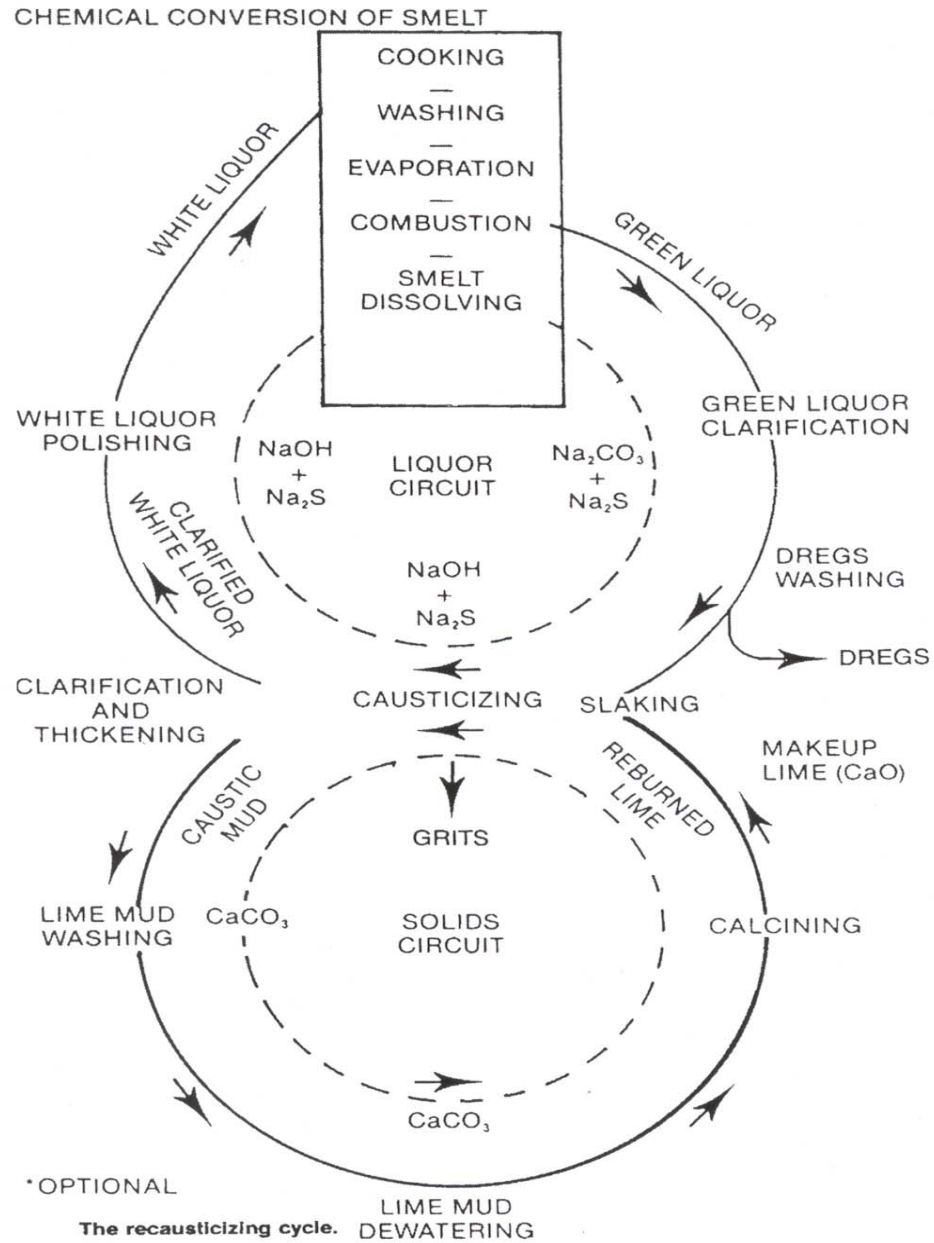


Figure 3: Chemical recovery cycle of the kraft process (3).

Prior Research

Two essential parameters for measurement in the kraft process are pulp yield and kappa number. Pulp yield is defined as the ratio of the bone dry weight of pulp to the bone dry weight of the original chips that were used to produce the pulp. Yield values in the kraft process can typically range between 30% and 70% depending on the cook conditions and whether or not the pulp is bleached for higher grades. Pulp yield can further be classified as total yield, screened yield, and bleach yield. Total yield is the actual yield of the pulp out of the digester and will always be the highest in value. Screened yield is the yield taken after the pulp has been screened to remove undigested wood components. Bleach yield is the yield of the screened pulp after it has been through the bleaching plant and is the lowest yield value measured in the process.

Kappa number is a measurement of the quality of the pulp and indicates the relative hardness, bleachability, or degree of delignification. Kappa number is defined as the volume of 0.1N potassium permanganate solution consumed by one gram of bone dry pulp (4). A fairly linear relationship is usually seen between the kappa number and the total yield of pulp. In the kraft process the control objective is to cook to a desired kappa number (1).

Kappa number of pulp is generally measured in an onsite lab, either manually or with an autotitrator. Manual tests generally follow the Tappi standard and the autotitrator is basically an automated form of this. These measurements can only be performed as quickly as a standard kappa test permits (~12 min) and do not allow for use as a process control parameter. Yield measurements are generally based on overall mass balances and are not accurate enough to allow for use as an online control tool. Mass balance

determinations suffer from raw material variability and many uncontrollable or immeasurable parameters in the process. Yield determinations may also be made through carbohydrate correlations which include the Marcoccia-Stromberg, cellulose, mannose and carbohydrate-lignin methods. However, these techniques require lab work and are not suitable for online control. Several optical methods have been examined for the measurement of kappa number and pulp yield. Using an optical type method offers the advantage of simplicity and relatively fast sampling time, which warrants their use as real time inline process control method.

The STFI (Swedish Pulp and Paper Research Institute) optical method has been implemented in process control for the measurement of kappa number. This system uses ultraviolet (UV) light absorption to quantify the lignin content of pulp. With this method pulp is sampled from the process and sufficiently washed and diluted. The fiber suspension is then illuminated with UV light and photodetectors measure the absorption. This determines the lignin content or kappa number independent of concentration. The washing process is a critical step for this analysis technique, since any dissolved lignin in solution would produce erroneous results. The system provides an accurate kappa number determination in about 5 min. This system has been in use in several mills, offering a reliable method with low maintenance (5). These systems are normally implemented before and after the bleaching stage and are only capable of measuring kappa number.

In another study, ^{13}C NMR, FTIR, and NIR have been compared in the measurement of carbohydrate (glucose and xylose) and lignin content of pulp derived from the kraft pulping of birch. Spectral data were collected for each method and analyzed using partial least squares (PLS) regression. In this comparison NIR

spectroscopy offered the best predictive ability of any single technique, but methods combining the data of all three resulted in even greater predictive ability (6). This result was also apparent in a similar study comparing only FTIR and NIR. Delignified samples of pine and sweetgum were tested for lignin, hemicelluloses, and cellulose composition. In this study, NIR was also found to be the superior method. Not only was the calibration more accurate, but also sample preparation and scan time were much faster (7). Additionally, a more recent study performed using photoacoustic FTIR spectroscopy along with PLS regression to find lignin and carbohydrate composition of hard and softwood pulps resulted in very accurate evaluation of composition, but suffered from a very high analysis time of 30-40 min per sample (8). The substantial time needed for this method eliminates it as a viable online measurement. Another study performed using FTIR, showed good predictability of kappa number and hexeneuronic acid of high-yield kraft pulp. This study also used the PLS regression method and made predictions on the region $1650\text{-}1200\text{ cm}^{-1}$ of the FTIR spectra which is in the longwave infrared region of the electromagnetic spectrum. This region was determined to contain characteristic bands of lignin and hexeneuronic acid (9).

Of the aforementioned spectroscopic methods, NIR appears to be the most suitable for implementation as an inline control tool. NIR correlations created with a multivariate regression technique offer good predictability of kappa measurements (10,11). It is also expected that NIR analysis can accurately predict pulp yield. Studies performed on wood meal using NIR measurements for the determination of cellulose content and pulp yield correlate very well with wet chemistry evaluations of these measurements (12,13). Although these experiments were performed with wood, similar

calibrations should be feasible using spectral data from pulp, as similar absorption trends should be seen in both the pulp and wood. Research has also been performed in modeling pulp yield using NIR measurements on higher yield pulps produced by semi-chemical pulping. In these studies, a strong correlation was found between NIR measurements and yield. It was also shown that this correlation could be applied to mill data giving good yield estimates. NIR was found to be a sensitive indicator of yield variation and machine runnability for the mill. The model was not as accurate for mills that used a blend of wood chip species (14).

NIR spectroscopy has been successfully implemented online in mills to measure the liquor component concentration and total dissolved solids of liquors (15). This alone is a very valuable control tool for pulp mills. With the addition of pulp yield and kappa information an unprecedented degree of control over digester operations may be possible. The evaluation of black liquor for lignin content and other components through NIR in addition to the NIR analysis performed on the pulp will allow the calibration of the NIR liquor analyzer for yield and kappa number, thus providing accurate predictions for control applications.

Very little work has been done for the development of online yield measurement. Few methods have been suggested and the difficulty in collecting samples that can be accurately analyzed is alone a substantial task. However, the use of near infrared (NIR) spectroscopy has proven to be a viable method for determining yield and kappa number. Good correlation between NIR absorbance and pulp yield and kappa number has been observed. This technique may prove to be sufficiently accurate for online control of digesters and have immense significance in the pulping industry.

BACKGROUND

Spectroscopy

Spectroscopy can be described as a measurement of amplitude and energy across a range of energies or frequencies. The device used to make these measurements and data set of measurements is referred to as a spectrometer and spectrum, respectively. Spectrometers come in many configurations and are employed in many diverse applications. Typically, optical spectrometers are the most abundant and have the widest range of applications. Optical spectrometers are available in many forms, including; transmission, attenuated total reflectance (ATR), and diffuse reflectance. These optical type spectrometers measure wavelength as the independent variable and percent transmission of radiation as the dependent variable. Some non-optical type spectrometers include acoustic spectrometers and electrical impedance spectrometers. Acoustic spectrometers measure the frequency of the acoustic wave against the attenuation of the wave and electrical impedance spectrometers measure voltage or current against electrical impedance (2).

The key advantage that all spectrometers have is the ability to make many measurements in a relatively short amount of time. The independent variable can cover thousands of measurements to produce a spectrum. Much technology is available to design and construct spectrometers that are optimized for specific conditions. Optically

based spectrometers in particular can, depending on the application, have rather simple designs and be built for a relatively low cost.

All types of spectrometers operate over some region of the electromagnetic spectrum. Figure 4 shows all regions of the electromagnetic spectrum. Optical spectrometers operate over a small region of the electromagnetic spectrum from 100nm to 40,000nm that includes ultra-violet, visible, and infrared regions. The infrared region of the electromagnetic spectrum is divided into short wave near infrared (SWNIR) 800nm to 1100nm, long wave near infrared (LWNIR) 1100nm to 2500nm, mid infrared (MIR) 2500nm to 4000nm, and long wave infrared (LWIR) 4000nm to 40,000nm.

Optical spectral methods are described mathematically by the Beer-Lambert relation. This relationship is described by the following equations:

$$\frac{dI(\lambda_j, x)}{dx} = -\alpha(\lambda_j, C_i)C_i I$$

Where $I(\lambda_j, x)$ is the output light (electromagnetic signal) intensity at wavelength λ_j at a distance x into the material, C_i is the molar concentration of i , and $\alpha(\lambda_j, C_i)$ is the absorption coefficient of i at wavelength λ_j . The equation is then integrated to yield the following relation:

$$I(\lambda_j) = I_0(\lambda_j)e^{-\alpha_{i,j}C_iL}$$

Where $I_0(\lambda_j)$ is the input light (electromagnetic signal) intensity and L is the length of material crossed by the light. The relation can be applied to a multi-component system by including a summation of components:

$$I(\lambda_j) = I_0(\lambda_j)e^{-\left(\sum_i \alpha_{i,j}C_i\right)L}$$

Additionally, the relation can be linearized for concentration changes:

$$A(\lambda_j) = \ln(I_0) - \ln(I) = L \cdot \sum_i \alpha_{i,j}C_i$$

Where $A(\lambda_j)$ is the linearized absorption at wavelength λ_j . Figures 5 and 6 illustrate the use of the Beer-Lambert relation as it applies to transmission and reflectance spectroscopy.

Optical spectrometers in general are composed of several components. A radiation source is generally projected onto the sample that covers a specific region of the optical spectrum. Transmitted or reflected light is sent to some type of dispersive element or filter, which subsequently filters out all but the desired wavelength or separates the light into its component wavelengths. The light is then sent to a photodetector which indicates the intensity of radiation of the transmitted or reflected light. Figure 7 shows a typical configuration of an optical spectrometer. All components involved are chosen and matched for their use over a particular region of the optical spectrum. Generally, different materials are used to produce components that operate optimally over the chosen region of spectral investigation.

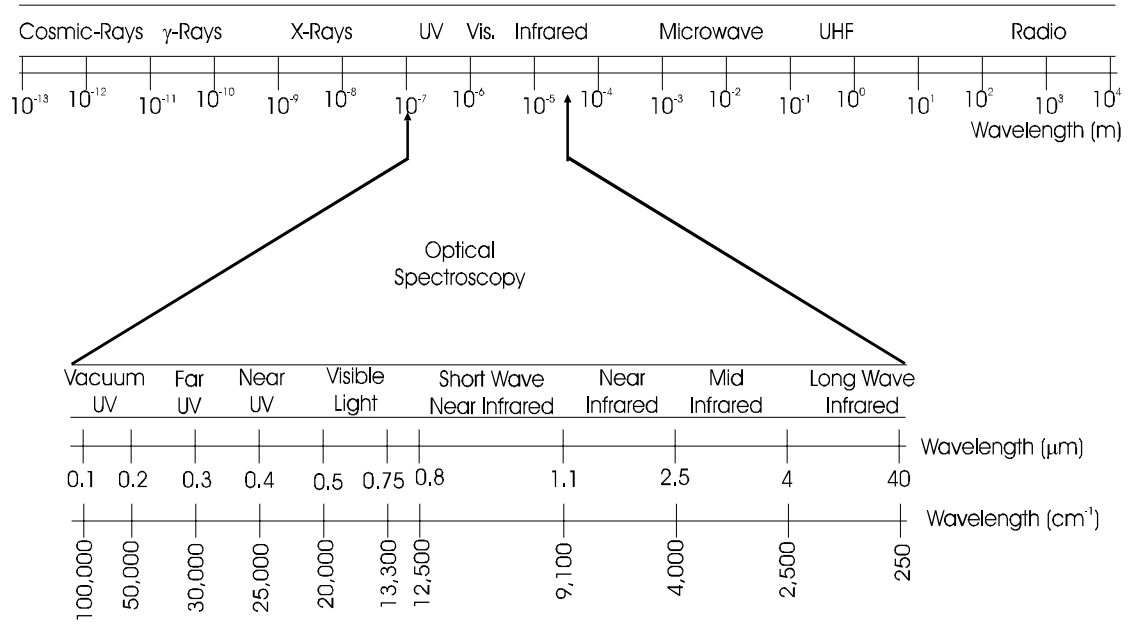


Figure 4: The electromagnetic spectrum.

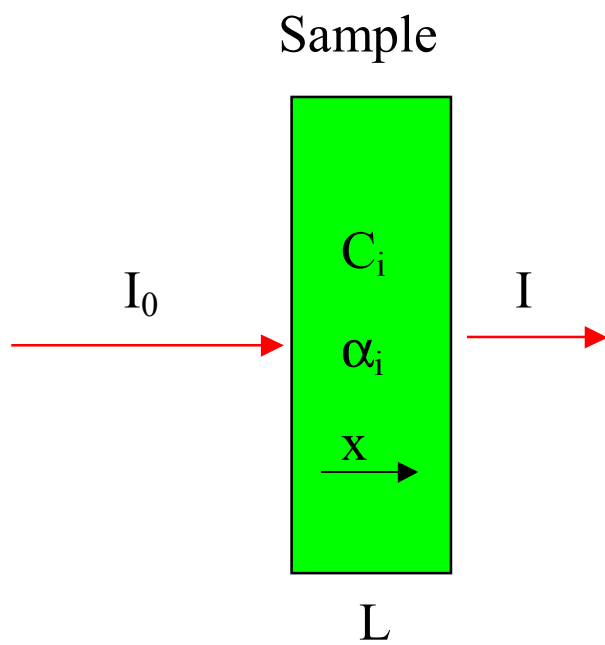


Figure 5: Variables for use with the Beer-Lambert relation in transmission.

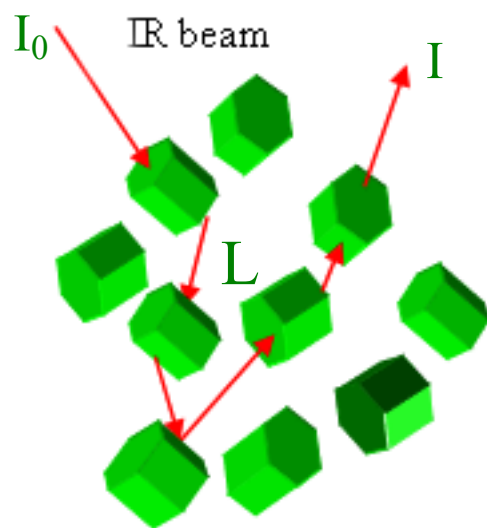


Figure 6: Variables for use with the Beer-Lambert relation in reflectance.

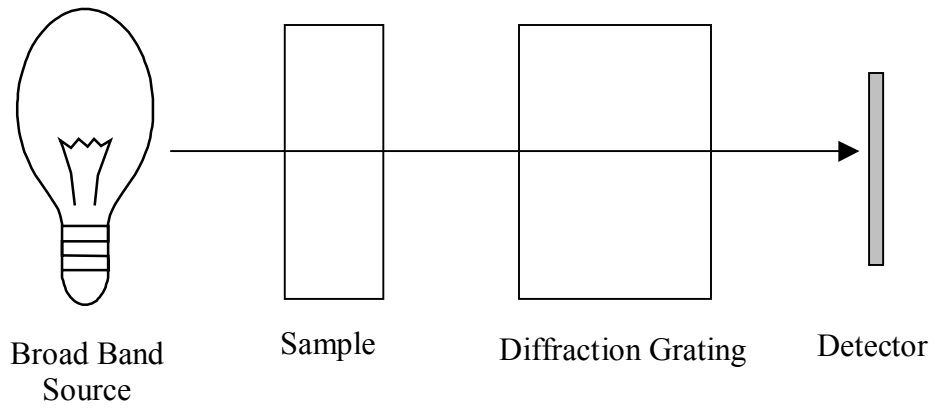


Figure 7: Typical optical spectrometer configuration.

Spectra Linearization

Spectra typically need to be linearized to correct for baseline offsets caused by variations in the contribution of the spectrometer and the environment in which the spectrum is collected. This can be done by collecting a reference spectrum that can then be used to linearize the actual spectrum of the sample. Spectra can be plotted in either transmittance or absorbance values, but absorbance is normally used for quantitative analysis because it is linearly proportional to concentration, whereas transmittance is not. The mathematics of the linearization is based on the aforementioned Beer-Lambert relation (16).

$$A = \log\left(\frac{I_0}{I}\right)$$

Where A is the absorbance, I_0 is the light intensity of the infrared beam measured with no sample (reference spectrum), and I is the light intensity of the infrared beam measured with a sample in place (sample spectrum).

The previous linearization is standard for spectra collected in a transmission arrangement, but may not be as accurate for reflectance spectra. With diffuse reflectance there may not be a direct relationship between peak intensity and composition of the sample. Diffuse reflectance does not have a fixed path length, unlike transmission, and peak intensities may be dependent on the depth to which the light penetrates the sample. Linearization of diffuse reflectance data may better be achieved through the use of the Kubelka-Munk function (17):

$$K_m = \frac{\left(1 - \frac{I}{I_0}\right)^2}{2\left(\frac{I}{I_0}\right)}$$

Where K_m is the corrected spectra, I is the sample spectrum, and I_0 is the reference spectrum. The Kubelka-Munk equation can be applied to diffuse reflectance to help linearize the spectrum to better correlate with concentrations or compositions of the sample. The equation corrects the spectral distortions created by a varying effective path length to produce a spectrum much like that of an absorbance transmission measurement.

Regression Techniques

Regression techniques are employed to relate spectral and chemical data for the development of calibration models and subsequent prediction of unknowns. Linear regression methods along with spectroscopy can be used for the development of these models. Three typical linear regression techniques commonly employed are Multiple Linear Regression (MLR), Principal Component Regression (PCR), and Partial Least Squares Regression (PLS).

Multiple Linear Regression

Multiple Linear Regression selects a small number of wavelengths to relate sample properties to spectral data. MLR applies a linear combination of responses to the independent variable that minimizes the error in determining the dependent variable. As long as there are few parameters that are not collinear and relate well to the responses, MLR proves to be a robust technique. Though with larger data sets and greater numbers of parameters, the data needed for identification becomes significantly large. Additionally, with the number of factors becoming greater than the number of observations the model tends to suffer from over-fitting and predictions become poor. MLR also tends to be very sensitive to noise in the spectra (18,19).

Principle Component Regression

Principle Component Regression identifies principal component scores of the dependent variable upon which the sample properties are regressed. This technique does not regress system parameters on the original measured variables, so it does not suffer

from the problems of large parameters sets associated with MLR. Basically, PCR determines variation related to the measured variable over the entire spectra. The algorithm of PCR involves a Principle Component Analysis (PCA) followed by a MLR of the component scores and measured variable values. The number of principle components that optimizes the model is determined through cross-validation. The use of PCR greatly reduces the number of parameters needed to build the calibration, making it more applicable to the analysis of spectral data sets (18,19).

Partial Least Squares Regression

Partial Least Squares Regression also uses the entire spectra, but further improves on the PCR technique. PLS not only determines principle components that explain variation in the independent variable, but also calculates principle components on the measured variables. A set of latent variables is chosen that maximizes covariance between the principle components of the independent and dependent variables. Essentially, these latent variables best define the properties of the spectra that relate to the measured values (20). This technique appears to be the most commonly used regression method for NIR spectroscopy and is the chosen technique for the research presented in this thesis.

Spectra Preprocessing

Several preprocessing techniques applicable to infrared spectroscopy have been developed. The goal is to transform the collected spectra in such a way as to make apparent the relation between the sample composition and the characteristics of the spectra. Ideally, spectral transformations should: correct for baseline offsets due to inconsistent sample presentation, reduce spectral variations for samples in the same class, increase the spectral differences between classes of samples, and linearize the response (18). Some mathematical techniques for achieving these transformations include: derivative methods, Savitsky-Golay smoothing and differentiation, discrete cosine transform low pass filtering, multiplicative scatter correction, standard normal variate scaling, orthogonal signal correction, mean centering, and slope and offset corrections.

Differentiation

Classic differentiation methods basically replace an absorption value at one wavelength by a difference in absorption values at adjacent wavelengths. Such derivative methods are generally available in mathematical and statistical software and they give similar results. The first derivative is usually applied to eliminate baseline offset variations within a set of spectra and the second derivative to eliminate slope variations.

Savitsky-Golay smoothing and differentiation allows for more options and is more sophisticated than classic differentiation techniques. Additionally, Savitsky-Golay does not increase the signal to noise ratio of the spectra, which occurs with classic differentiation. Savitsky-Golay operates on a specific window of the spectra determined by the user. The algorithm fits a polynomial over the window incrementally across the

entire spectrum. An estimate of the derivative of the function is calculated from the fit giving a smoothed function.

Filtering

A discrete cosine transform (DCT) can be used to filter noise out of a spectrum. The transform of the spectra is taken with the number of points kept in the DCT domain optimized to retain all the pertinent spectral information. An inverse DCT of the data is then performed to return the filtered spectra. The DCT function is described mathematically as follows:

$$H(u, v) = \frac{2}{\sqrt{MN}} C(u)C(v) \sum_{x=0}^{M-1} \sum_{y=0}^{N-1} h(x, y) \cos\left[\frac{(2x+1)u\pi}{2M}\right] \cos\left[\frac{(2y+1)v\pi}{2N}\right]$$

the inverse DCT:

$$h(x, y) = \frac{2}{\sqrt{MN}} C(u)C(v) \sum_{x=0}^{M-1} \sum_{y=0}^{N-1} H(u, v) \cos\left[\frac{(2x+1)u\pi}{2M}\right] \cos\left[\frac{(2y+1)v\pi}{2N}\right]$$

where,

$$C(\gamma) = \begin{cases} \frac{1}{\sqrt{2}} & \text{for } \gamma = 0 \\ 1 & \text{for } \gamma > 0 \end{cases}$$

Signal Correction

Standard normal variate (SNV) scaling and multiplicative scatter correction (MSC) are techniques designed to deal with varying path lengths of samples in a data set, due to scattering effects associated with diffuse reflectance. SNV uses a fairly simple approach where each spectrum in a data set is mean centered and then divided by its

standard deviation. MSC first calculates a mean spectrum based on all the spectra in the data set. Next each spectrum is regressed against the mean spectrum providing a linear equation with a defined intercept and slope. Then the intercept is subtracted from each point in the spectrum and the resulting absorbance is divided by the slope. This minimizes variations in the spectra not related to sample composition. SNV and MSC tend to give fairly similar results when applied to the same set of spectra (21). These techniques both tend to align spectra of samples with similar composition.

Orthogonal signal correction (OSC) is another method intended to correct light scattering effects. OSC is unique in that it uses measured sample values in its algorithm. OSC is designed to remove variations in the spectra unrelated to the sample property values. The algorithm computes a matrix of weights that are used to determine variance in the predictor block unrelated to the predicted block. This component is then subtracted from the predictor block. This technique is used in conjunction with PLS modeling. The weights are determined for the calibration set and then applied to new spectra for prediction. This technique gives very good calibration plots and can be helpful when transforming a calibration for use with a new spectrometer that the calibration was not originally built with.

EXPERIMENTAL METHODS

Overview

The development of models for calibration and prediction of kappa and yield values required several steps. Pulp samples had to be created and lab tested for kappa number and yield. A reflectance set-up for use with the spectrometer had to be developed, fabricated, and optimized. In some cases the actual spectrometer had to be built and tested. Additionally, many permutations of spectra transformations had to be investigated to create the best models. The scope of this project was not necessarily to develop these models with the most robust lab techniques available for NIR spectroscopy, but to utilize techniques and technology developed by the third party company. A prototype spectrometer has been developed that is relatively simple and inexpensive, but is capable of being implemented in laboratory as well as inline industrial applications. The methods used in this research were always implemented with great consideration to their applicability to mill situations.

NIR Spectroscopy

NIR spectroscopy was utilized during the course of this research. NIR spectroscopy focuses on the study of the interaction of light in the NIR region with some medium (22). NIR spectroscopy has many key benefits. This technique is universal and much technology has been developed for its application. The spectra provide immense information for determining the composition of samples and correlating their identities. The locations of peaks and their general shape and size can be used to identify functional groups or measure concentrations. Most importantly for online applications, NIR spectroscopy is a relatively fast, simple, and inexpensive method of analysis (22).

Transmission and diffuse reflectance type NIR spectrometers are examined in this research. Transmission configurations are best for liquids and can be easily employed for the analysis of black liquor. For a transmission spectrometer the radiation source is projected onto the sample and the transmitted light is collected and analyzed. Diffuse reflectance configurations are used for the analysis of pulp samples because of their applicability to light-diffusing medium such as a roughened or uneven surface. For diffuse reflectance the radiation source is projected onto the solid sample and the diffusely reflected light is collected and analyzed.

Sample Preparation

A total of three sets of pulp samples, referred to as A, B, and C, were prepared during the course of this research. Data for the pulp samples can be found in Appendix A. The preparation of each consecutive sample was optimized to deal with potential variability in samples that may have been the cause of poor kappa and yield models. For sets A and C only pulp was collected, but for set B the spent black liquor was also collected for analysis and investigation into its correlation with pulp yield and kappa number using NIR spectroscopy.

For all of the sample sets, southern pine pin chips were cooked over a broad range of conditions to give a good spread of kappa and yield values. Mill wood chips were used to make the pin chips by first allowing them to air dry and then shredding them in a heavy-duty blender. The shredded chips were then sifted to separate the fines and larger chips. This process produced pin chips of fairly consistent size that were sufficiently small for cooking in stainless steel bombs. On average, the pin chips were 1mm in width and 15mm in length. The bombs used for cooking in sample sets A and B were 50mL capacity and those used for set C were 500mL capacity. Figure 8 shows a comparison of the two different size bombs. The bombs were immersed in water inside a lab batch digester for cooking.

For the cooks, liquor to wood ratios was approximately 5.0, with a 9.0g charge of wood chips in the 50mL bombs and 90g of chips for the 500mL bombs. The use of individual bombs allowed for the quantitative determination of pulp yield and the quick generation of many pulp samples with a wide range of characteristics. Cooking liquors of varying effective alkali (EA) from 30 g/L to 110g/L as Na₂O were used in the cooks.

In sample sets A and B mill white liquor with an EA of 110 g/L as Na₂O was diluted to achieve the different concentrations of liquor used for cooks. For set C, synthetic liquor was produced by dissolving appropriate amounts of NaOH and Na₂S in water.

Additionally, cook times of 0.5 hours to 2.5 hours in 0.5-hour increments and cook temperatures of 160, 165, and 170°C were used.

In the sample set A, three bombs were used at each set of the conditions thereby producing triplicate for each sample. However, this did not allow for enough pulp to determine a repeatable kappa number, yield value, and allow for enough sample for the NIR analysis. For this reason sample set B employed the use of six 50mL bombs per sample condition which provided plenty of pulp for analysis. For sample set C the larger 500mL bombs were used so that pulp at a particular condition all came from the same bomb. When using several bombs at the same condition, the pulp from each bomb was mixed and kappa and yield values were then determined and treated as one sample. Even though each bomb at a particular condition was given the same treatment as far as liquor EA value and cook time and temperature, it was speculated that there may have been slight discrepancies in measured values from bomb to bomb. It is for this reason that the larger bombs were used to produce sample set C. The use of larger bombs inherently increases the accuracy of yield measurements as well. This is because small amounts of pulp that may be lost during washing are much less significant to the calculation when using bombs that are an order of magnitude larger.

After cooking, the pulp was washed by running tap water over the digested chips residing in a Buchner funnel with a vacuum applied. For sample set B the spent black liquor was collected from a few bombs and a sample of all the liquor and washings was

collected from one of these bombs and diluted to 2000mL for each sample. It was hypothesized that collecting the diluted washing set would allow for analysis of the entire volume of components in the liquor.

Once the pulp was thoroughly washed (i.e. the wash water was fairly clear), the chips were put into a blender to blow them apart into pulp fibers. The pulp was then poured into a Buchner funnel with filter paper and the water was vacuumed out, thereby forming the pulp pads that were to be used for analysis. The pads were all air-dried and the total weight for a sample was determined. A small amount of the sample was then oven-dried for the moisture determination. An average yield for each sample was determined and the yield values ranged from 31% to 67%. The air-dried samples were sealed in bags and were later used for NIR analysis and kappa testing.

Kappa tests were performed according to the Tappi standard (4). To ensure good repeatability, initial kappa test were performed to determine the approximate kappa number, usually two to three, then an additional two to three kappa tests were performed and an average kappa value was computed from these. Generally, consecutive kappa tests provided values that were within 0.5 units of the average value. Kappa numbers ranged from 13 to 100 for the pulp samples.



Figure 8: Bombs used during the cooking process.

NIR Analysis

The pulp samples were analyzed using an NIR spectrometer and reflectance set-up for collection of the spectra. The black liquor samples used a NIR spectrometer and transmission set-up. The best configuration for the transmission set-up was clearly defined, but the reflectance arrangement required several iterations of the design. Additionally, three different spectrometers were utilized for the collection of reflectance spectra of the pulp samples. The three spectrometers used included a Rosemount AOTF-NIR Analyzer and two prototype analyzers. The spectral data was sent to a computer and appropriate software was used to visualize the spectra and organize the absorbance values into a spreadsheet. Figure 9 shows a graphic of the typical set-up used for collection of the NIR spectra.

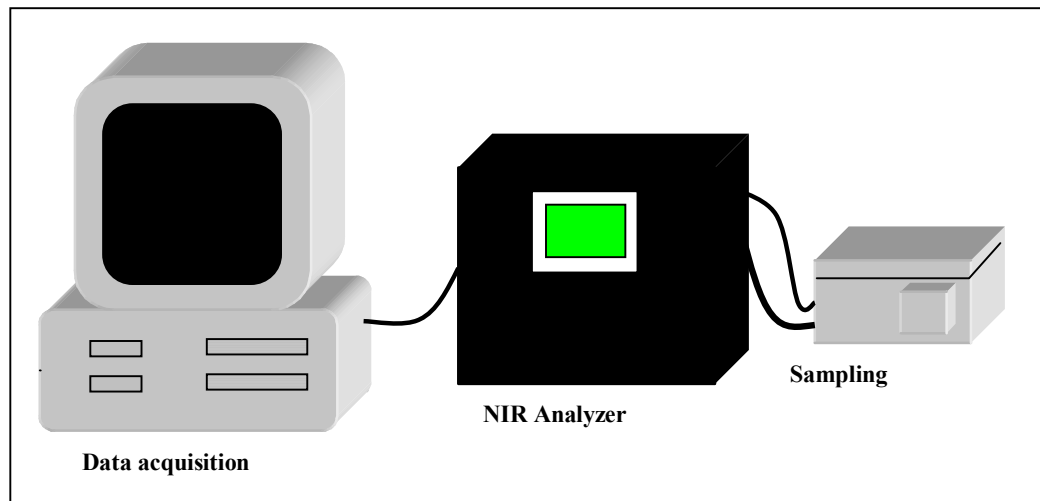


Figure 9: Data collection system.

The transmission set-up for the collection of black liquor spectra is fairly simple. A holder is used that the light source and light collector are affixed to. The liquor sample is injected into a 1mm quartz cuvette and placed between the light source and collector on the holder. The 1mm pathlength has been proven by other studies to be a good arrangement for analyzing black liquor. The sample is illuminated and the transmitted light is collected and sent to a spectrometer via fiber optic cable. Figure 10 shows the configuration for the collection of the transmission spectra of the black liquor. The prototype spectrometer used scans in the long wave near infrared region from 1000nm to 2200nm and was built and designed by a third party company.

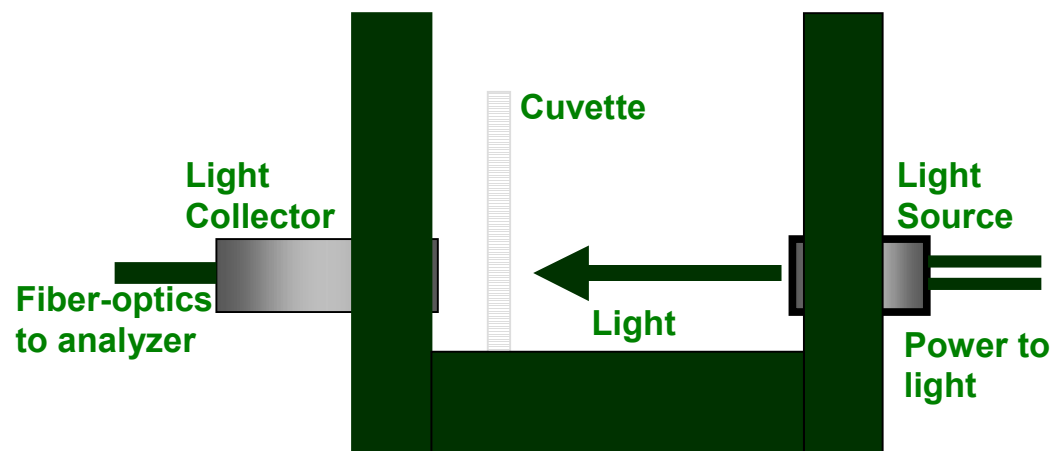


Figure 10: NIR transmission set-up.

Sample set A was used as a preliminary analysis of kappa number and yield predictions using NIR spectroscopy. A basic reflectance set-up was fabricated for the collection of the spectra. Pulp samples were pressed into a circular sample holder and the light source and collector were placed at a 45° angle in relation to the sample. A hand press was fabricated to press the pulp into the sample holder. By pressing the samples most of the water was allowed to drain out and the pulp retained about 20% moisture. Figures 11 and 12 show pictures of the hand press and reflectance set-up used to accomplish the aforementioned sample presentation. The sample spectra were collected using an acousto-optic tunable filter (AOTF) NIR analyzer built by Rosemount. This analyzer used a wavelength range from 1058nm to 2115nm and 256 absorbance values were recorded in this range. Figure 13 shows a picture of the entire system used.

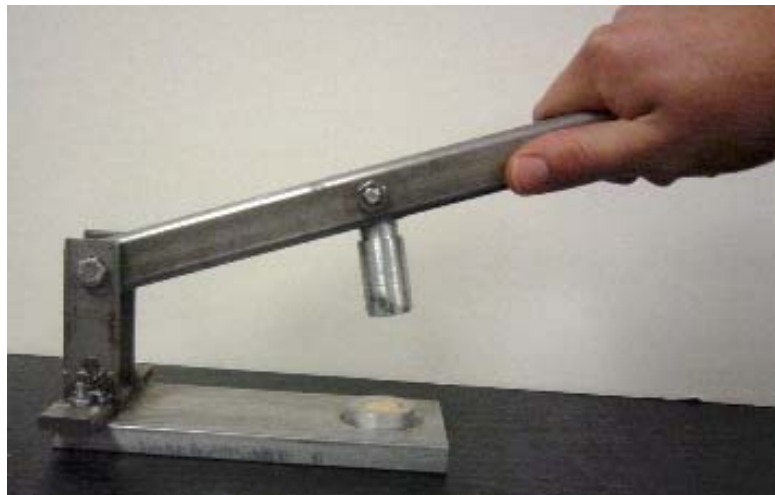


Figure 11: Hand press for sample preparation.



Figure 12: Reflectance set-up.

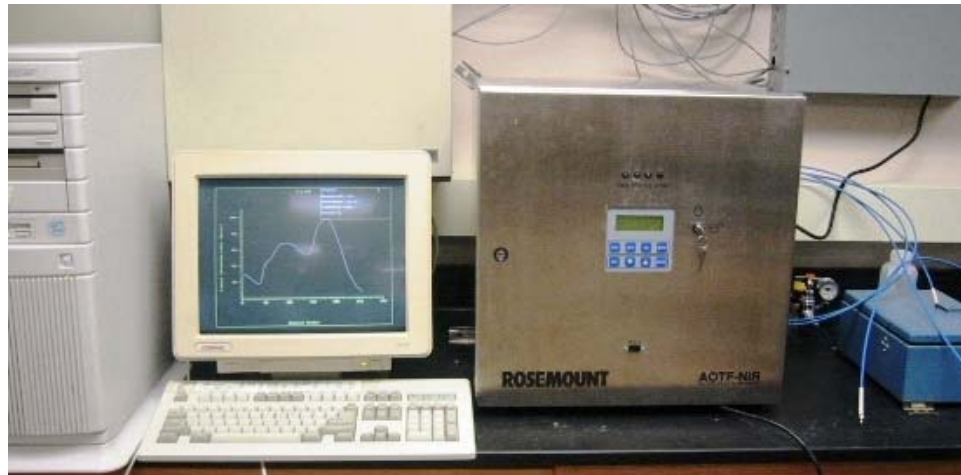


Figure 13: Rosemount AOTF-NIR system.

Spectra for sample set B were collected using a modified reflectance arrangement and spectrometer. For this reflectance arrangement, pulp samples were placed in an aluminum holder with a sapphire window through which the reflectance measurement was made. The pulp first dispersed in water and pressed into the sample holder such that pulp was pressed flat against the sapphire window to allow ample presentation for reflectance. Figure 14 shows the orientation of this reflectance set-up. Once again sample moisture was about 20% and a sufficient amount of pulp was used to produce a thick layer of pulp to ensure the light did not penetrate the entire depth of the sample. A Teflon reference was also used between scans in order to produce consistent spectra and eliminate spectral changes due to light source variations.

The reflectance spectra of the samples were collected with a prototype NIR spectrometer designed for mill use by a third party company. Spectral data was transferred from the spectrometer to a PC via ethernet connection. Figure 15 shows a photo of the prototype NIR analyzer. The samples were scanned over a wavelength range of 1200-2100 nm and absorbance values were recorded at 0.9375 nm increments. This allows for sufficient detail in the spectra.

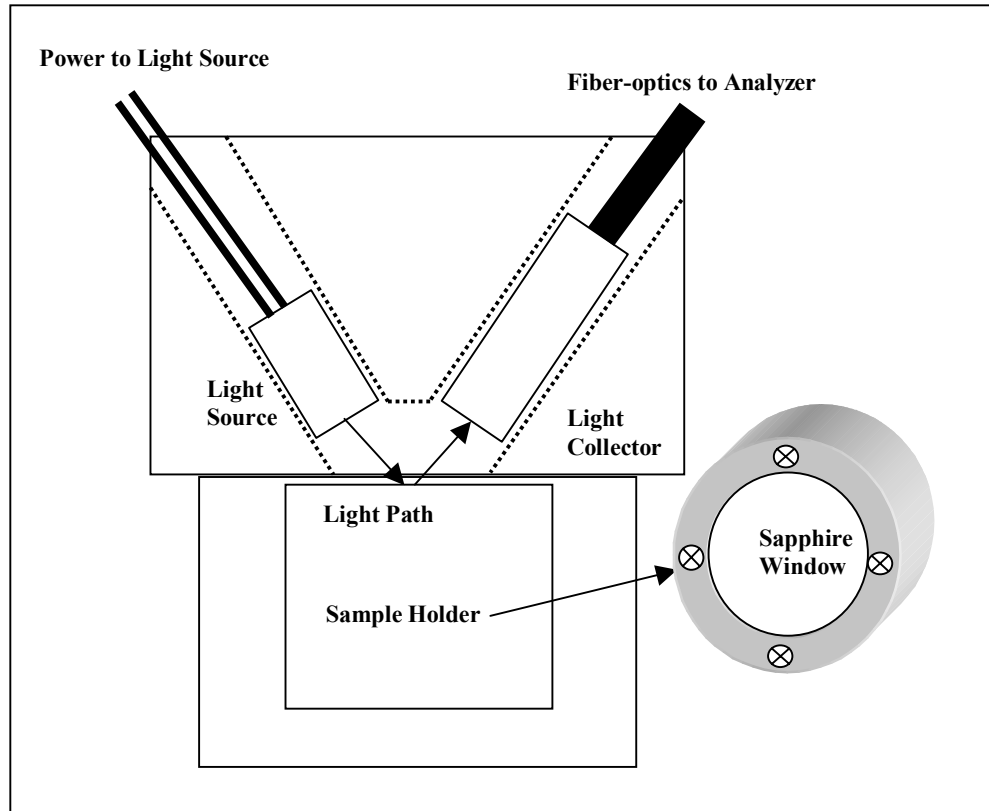


Figure 14: Reflectance set-up.

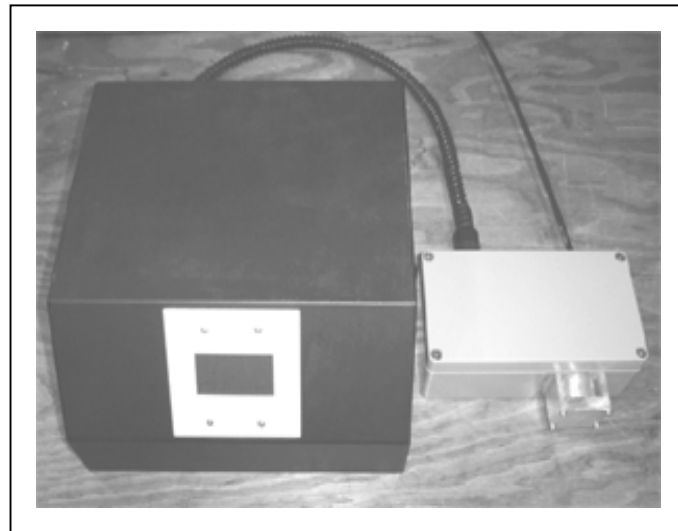


Figure 15: Prototype spectrometer.

For sample set C another method of sample presentation and reflectance orientation was used. The reflectance orientation was similar to the previous set-up shown in figure 14, but pulp samples were prepared by pouring slurry containing approximately 8g of air dried pulp into a Buchner funnel and vacuuming for 1 min. The pulp pad was then placed on top of the reflectance set-up and subsequently scanned. This method generally resulted in about the same pad moisture content as the previous methods, but was thought to give a more uniform pulp pad for analysis. Two different prototype spectrometers were used for analyzing sample set C. One used an optical bench designed to scan the short wave NIR region from 830nm to 1660nm at 1nm increments. The other bench was designed for long wave NIR and scanned in a range from 1000nm to 2200nm at .9375nm increments. The key differences in these optical benches were the monochromator and photodetector used. Both of these elements had to be chosen according to the region of the NIR spectrum in which they were utilized.

Three scans of each sample were taken consecutively where the pulp pad was repositioned on the reflectance set-up for each consecutive scan. By repositioning the pad it is possible to determine variability in the spectra caused by characteristics of the packing of the pulp and variations in the surface of the pad. An air reference was also taken for each sample before the pulp pad was scanned. Figures 16 and 17 show a picture of the analyzer and final reflectance set-up used for the collection of spectra on sample set C.



Figure 16: Picture of prototype spectrometer.



Figure 17: Picture of reflectance set-up.

Software

Different software packages were utilized for the collection and analysis of the spectra. Spectracalc software was used for the collection of spectra using the AOTF-NIR analyzer. Software developed by a third party company was used for the collection of spectra analyzed using the different prototype spectrometers. Both of these software packages organized the absorbance values of the spectra into a spreadsheet that could be loaded into additional software for analysis. Matlab was used as the primary tool for processing the spectra and building models for calibration and prediction. A PLS toolbox developed for use with Matlab by Eigenvector Research Inc. contained the specific algorithms used for analysis. The algorithms come in the form of Matlab m.files and contain code used to accomplish the PLS and various spectral preprocessing. Also, other Matlab m.files were created for the organization of the spectra and some of the preprocessing. The code for these m.files is shown in Appendix B.

The spectral data collected from the analyzer was extracted in the form of a text file and loaded into Matlab as a matrix. The matrix is then organized into an $M \times N$ matrix of M wavelengths and N absorbance values. The spectra were first linearized using either the Beer-Lambert relation or the Kubelka-Munk equation in conjunction with the sample spectra matrix and a reference matrix of the same size. The output was a linearized matrix of the same size as the sample and reference matrix. All spectral preprocessing techniques were then directly applied to the linearized matrix. The PLS regression is then applied to the preprocessed matrix and a corresponding matrix of measured values. The resulting independent and dependent variable loadings, independent variable weights and inner relation coefficients from the PLS regression are

then applied to a matrix of spectral data of unknown samples for prediction. The PLS model then returns a matrix of predicted values for the unknown samples.

RESULTS AND DISCUSSION

Overview

The goal of this research was to determine the ability to estimate pulp yield and kappa number from NIR spectral information using technology developed by a third party company. Correlation of kappa number and pulp yield with both pulp reflectance spectra and spent black liquor transmission spectra were considered. Essentially, the approach is to accurately determine lab values for the measurements of interest, collect spectra with detailed information, determine necessary data preprocessing to get the most information from the spectra, and build accurate calibration models that can predict the kappa and yield values of unknown samples. This methodology was applied to all collected data sets. The data sets include: spectra of sample set A collected with the Rosemount AOTF-NIR analyzer, spectra of sample set B collected with the prototype LWNIR analyzer, and spectra of sample set C collected with both the prototype LWNIR and SWNIR analyzer.

Characteristic Spectra

Every spectrometer has its own characteristics that affect the appearance of the spectra it generates. Even when the same design and fabrication process is used, slight variations may be seen in spectra from one spectrometer to the next. Variations in the light source and how the light interacts with the sample can cause discrepancies in spectral measurements. For example, figure 18 shows spectra collected with the same prototype optics bench, the only difference between the two groupings was the use of different light sources. Even though the light sources were the same model, slight nuances in the orientation of the filament may have led a change in the absorption values and variations in the spectra. Fortunately steps can be taken to adjust calibrations built with one spectrometer to be applied to another.

Three different spectrometers were used during the course of this research. A Rosemount AOTF-NIR spectrometer was used with the sample set A as a preliminary investigation into the potential of NIR as a method for predicting kappa and yield values. The Rosemount analyzer's operating range was from 1058nm to 2115nm. Figure 19 shows some typical spectra from the Rosemount analyzer representing samples with kappa numbers ranging from 13 to 100 and yields ranging from 35% to 70%. Spectra from this analyzer are not as detailed as those of the prototype spectrometers, because the absorption is only measured about every four wavelengths. However, the signal to noise ratio is relatively high.

Further analysis on sample sets B and C was performed using two similarly designed prototype spectrometers, one optimized for short wave NIR and the other for long wave NIR. The prototype SWNIR spectrometer covered wavelengths from 830nm

to 1660nm, while prototype LWNIR spectrometer covered wavelengths from 1000nm to 2200nm. Figures 20 and 21 show typical spectra from the SWNIR and LWNIR spectrometers, respectively. These spectra represent samples with kappa numbers ranging from 13 to 100 and yields ranging from 35% to 70%. There is a sizable overlap in the spectral region for both of these prototype analyzers. As a result, spectra collected on one analyzer may prove to contain more pertinent information for building calibrations. Calibrations need to be evaluated for both spectra to determine which spectrometer yields the best predictive ability. SWNIR has much less noise associated with the spectra than does LWNIR due to the type of photodetector used. If the SWNIR spectra contain the necessary information to create a good calibration model, the method would be superior to LWNIR because of the higher signal to noise ratio.

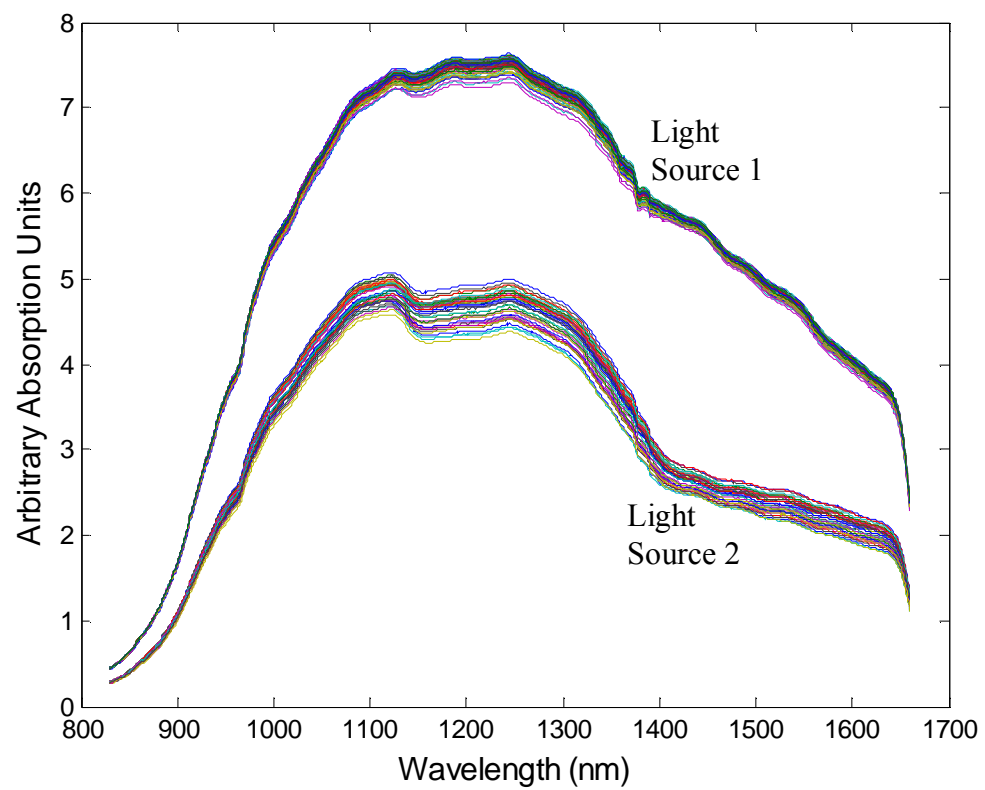


Figure 18: Spectra collected using different light sources.

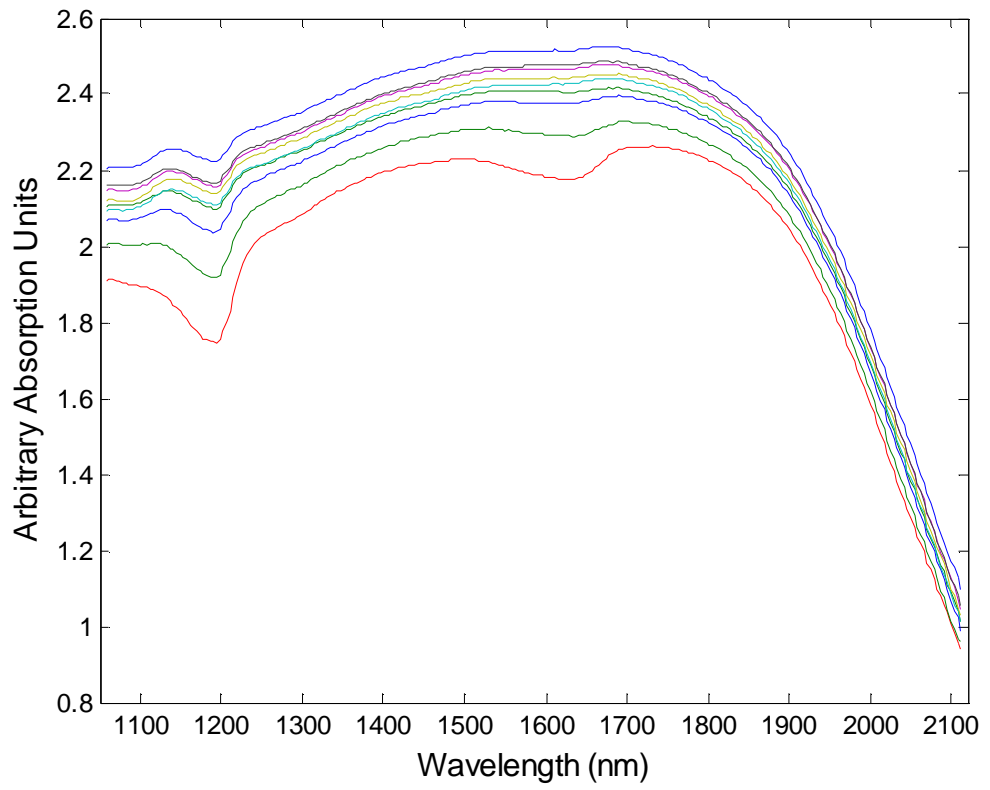


Figure 19: Spectra of pulp from the Rosemount AOTF-NIR spectrometer.

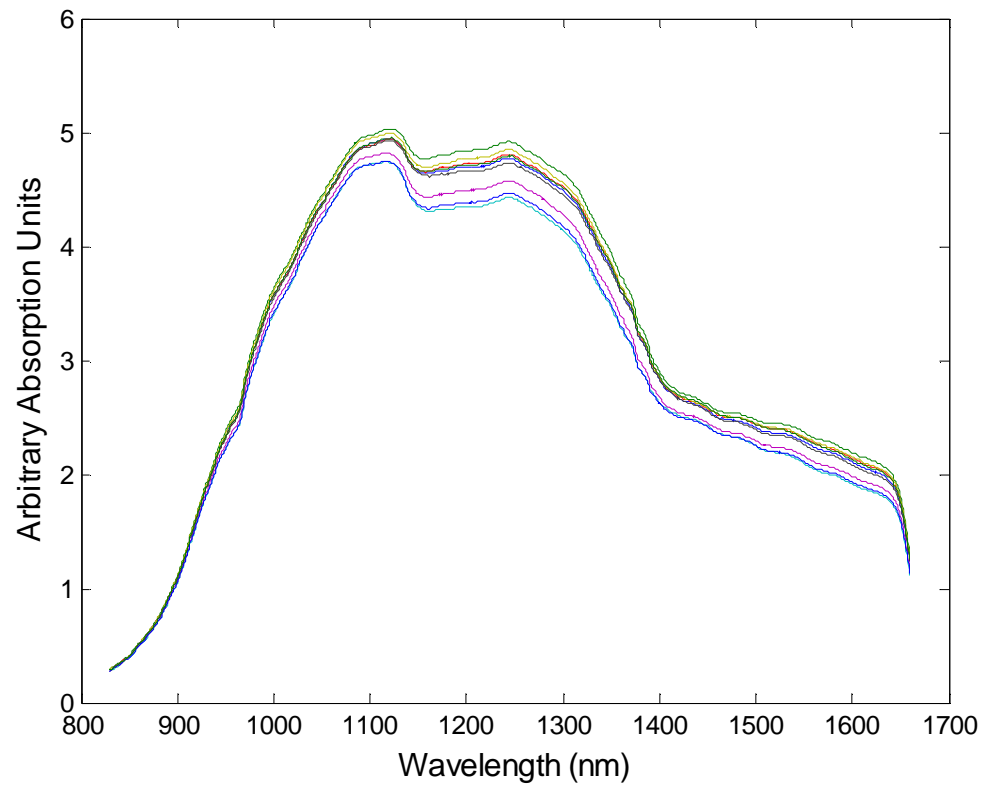


Figure 20: Spectra of pulp from the SWNIR prototype spectrometer.

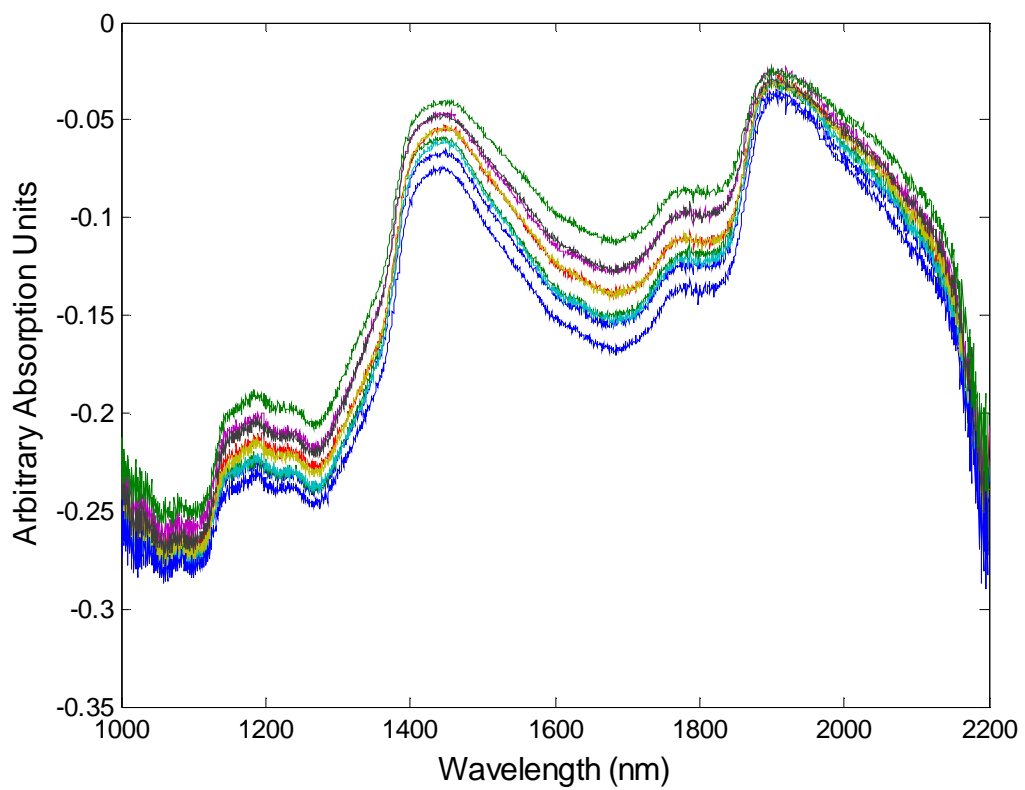


Figure 21: Spectra of pulp from the LWNIR prototype spectrometer.

Spectra Smoothing and Differentiation

Considering the previous spectra the level of noise can vary considerably depending on the type of spectrometer used. Electronic noise can be reduced through design considerations when building a spectrometer, but in some instances high levels of noise may be unavoidable. It was found that there is a relatively low amount of light throughput associated with the reflectance pulp spectra collected during the course of this research. To deal with this, the signal from the photodetector was amplified considerably with the prototype spectrometers. Unfortunately, amplifying the signal also increases the noise in the spectrum. This becomes more of an issue with spectra collected on the LWNIR analyzer due to its inherently noisier components. Figure 22 shows a close up of some raw spectra from the LWNIR analyzer. There is a consistent noise shown in this figure which most likely corresponds to every increment of the stepper motor that turns the grating in the monochromator of the spectrometer.

To deal with the inherent noise of the spectra, filtering or smoothing was employed by applying these techniques to different degrees and qualitatively comparing the resulting spectra. Discrete cosine transform filtering proved very useful for smoothing the spectra. It was very simple to adjust the amount of filtering in order to retain the pertinent information in the spectra. Figures 23, 24, and 25 show unfiltered spectra, spectra with very little filtering, and spectra with considerable filtering, respectively. The spectra with the most filtering still retained 99.9% of the signal, but using a small amount of filtering may be sufficient, and can produce spectra that can be further processed by differentiation. On the other hand, if a standard derivative is taken of a fairly noisy spectrum the noise will be considerably amplified. Figure 26 shows the

first derivative of a raw spectrum from the LWNIR analyzer. It is obvious that no useful analysis can be made with this spectrum. If DCT filtering is first applied to the spectra and a derivative is taken a considerably more useful spectrum can be realized as shown in figure 27.

Through qualitative comparison the Savitsky-Golay smoothing and differentiation method proved to be superior method to the aforementioned DCT filtering followed by differentiation. Although, some minor DCT filtering might first be employed before Savitsky-Golay for a considerably noisy spectrum. For most of the calibration models a second-order polynomial and first derivative with a modest window size was used with the Savitsky-Golay algorithm. Figure 28 shows a Savitsky-Golay treated spectrum of the same sample as in figure 27. The Savitsky-Golay algorithm produces a much cleaner spectrum. Figures 29, 30, and 31 show Savitsky-Golay treated spectra from all three aforementioned spectrometers. These spectra have well defined peaks and taking the first derivative helps remove baseline offset and other variations caused by inconsistent moisture content from sample to sample.

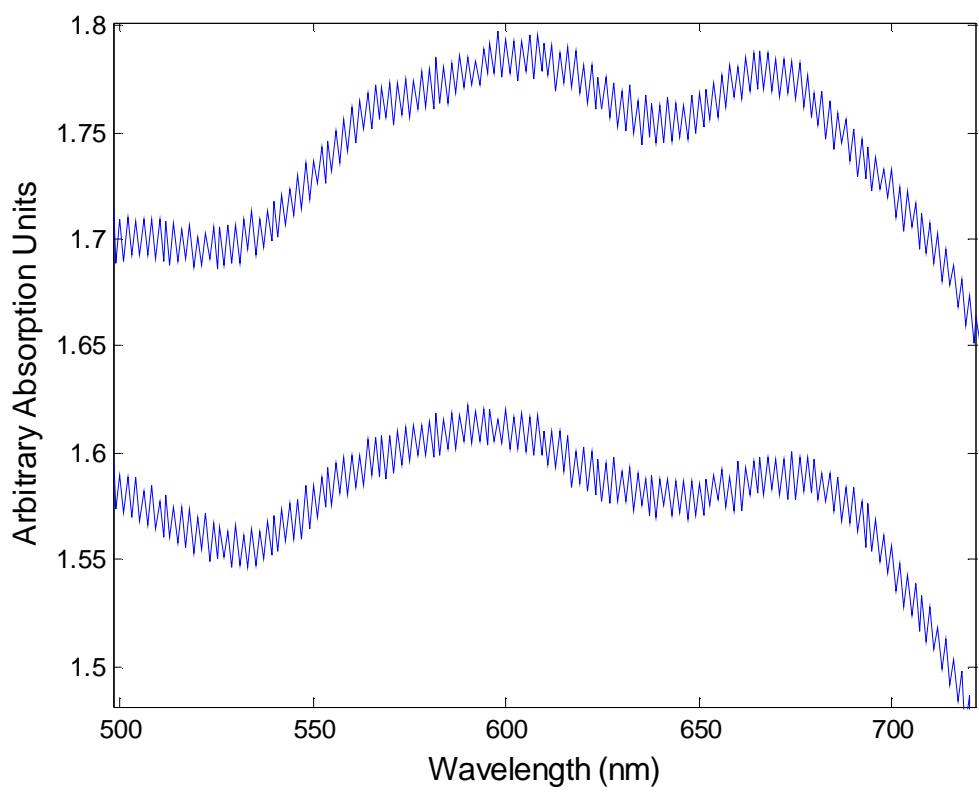


Figure 22: Oscillations in spectra caused by motor noise in the LWNIR analyzer.

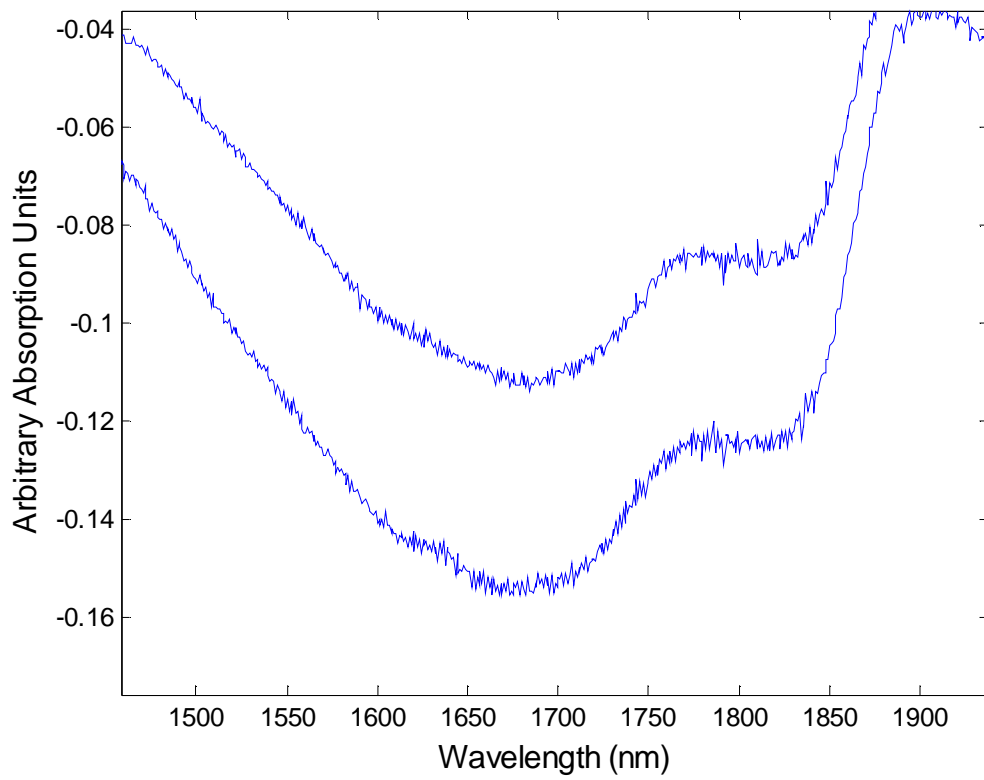


Figure 23: Close-up of unfiltered spectra from the LWNIR analyzer.

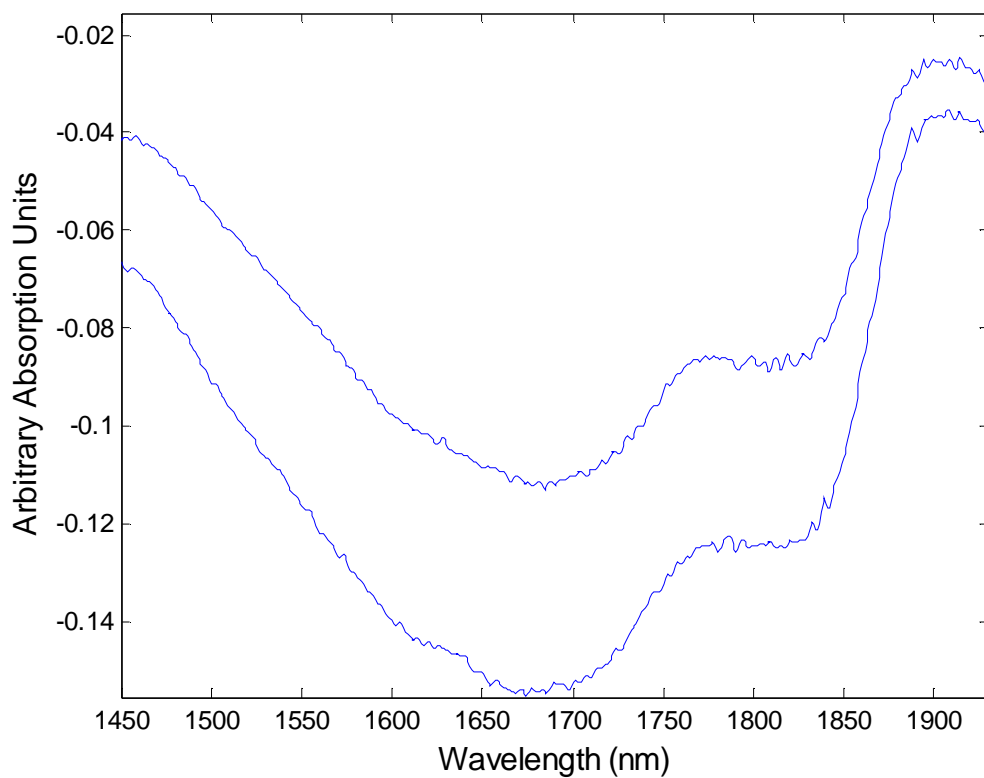


Figure 24: Spectra from the LWNIR analyzer with some DCT filtering.

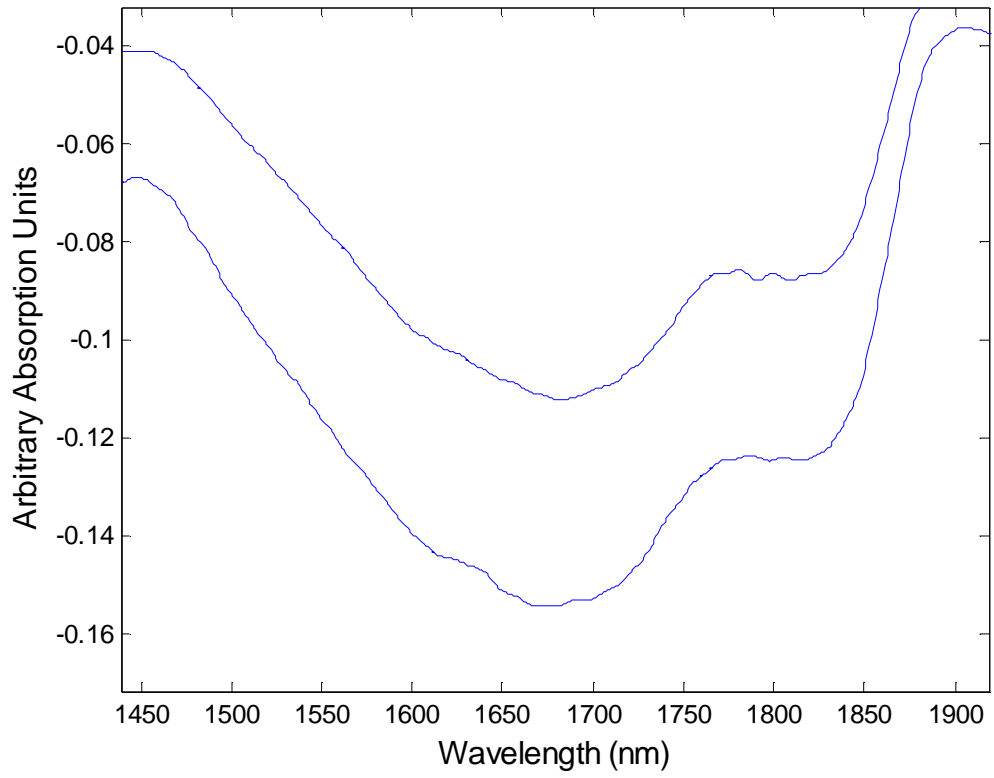


Figure 25: Spectra from the LWNIR analyzer with considerable DCT filtering.

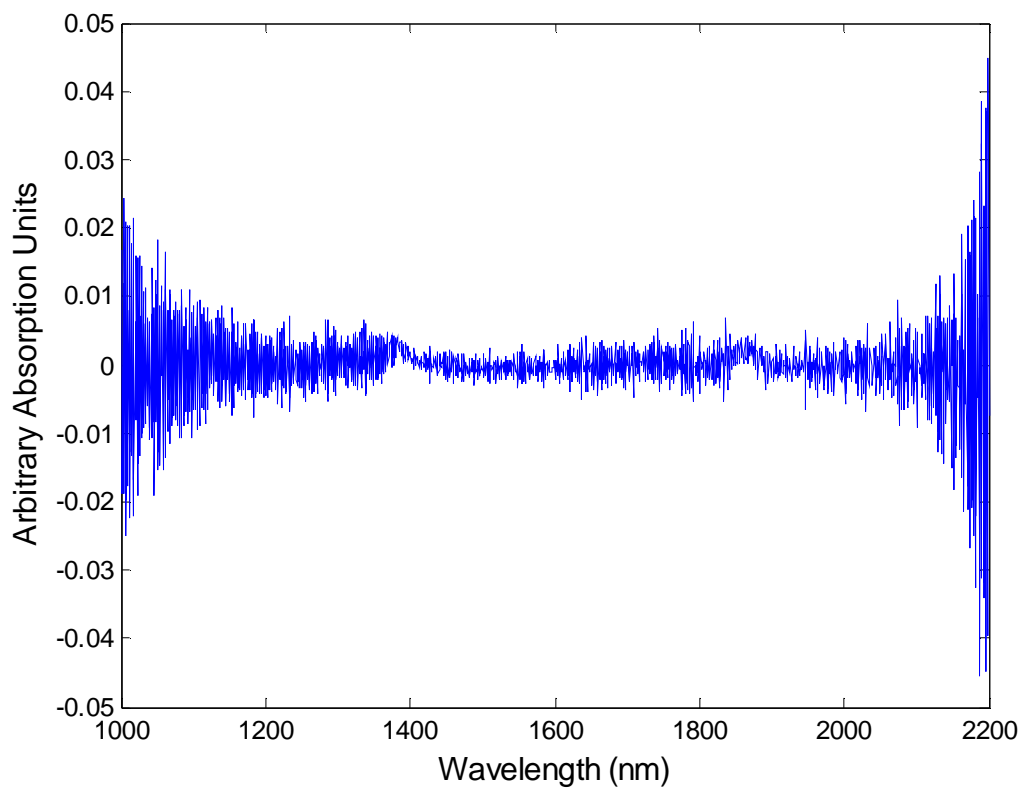


Figure 26: First derivative of raw spectrum from the LWNIR analyzer.

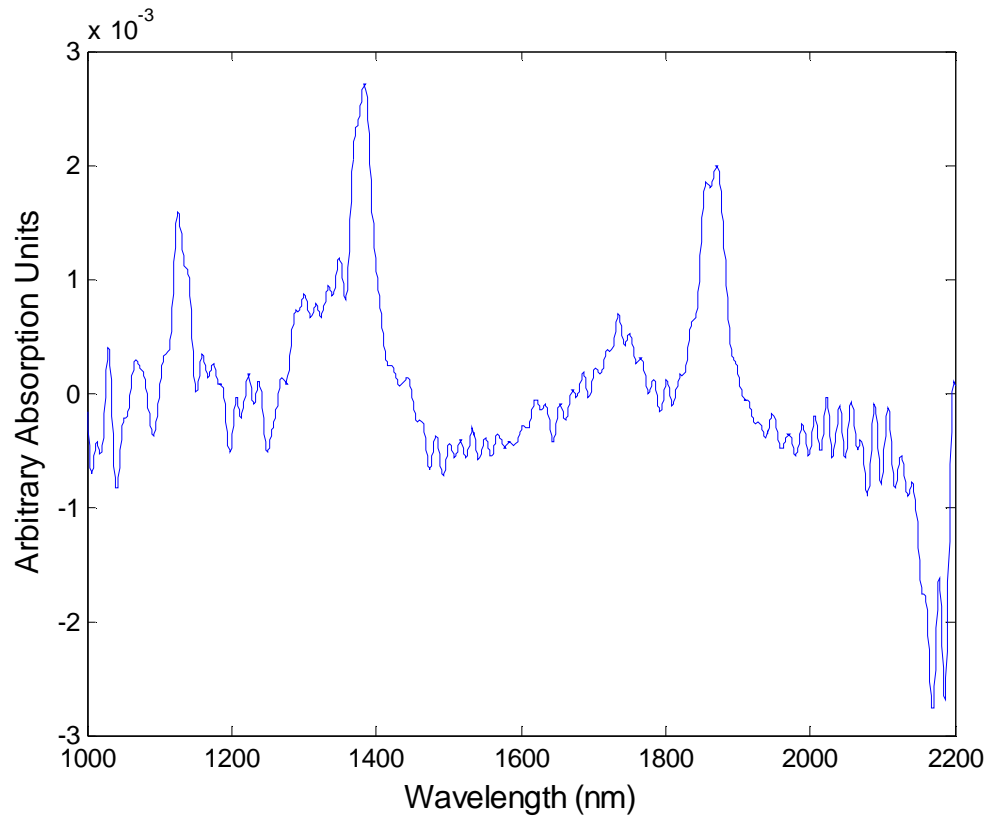


Figure 27: DCT filtered and differentiated spectrum from the LWNIR analyzer.

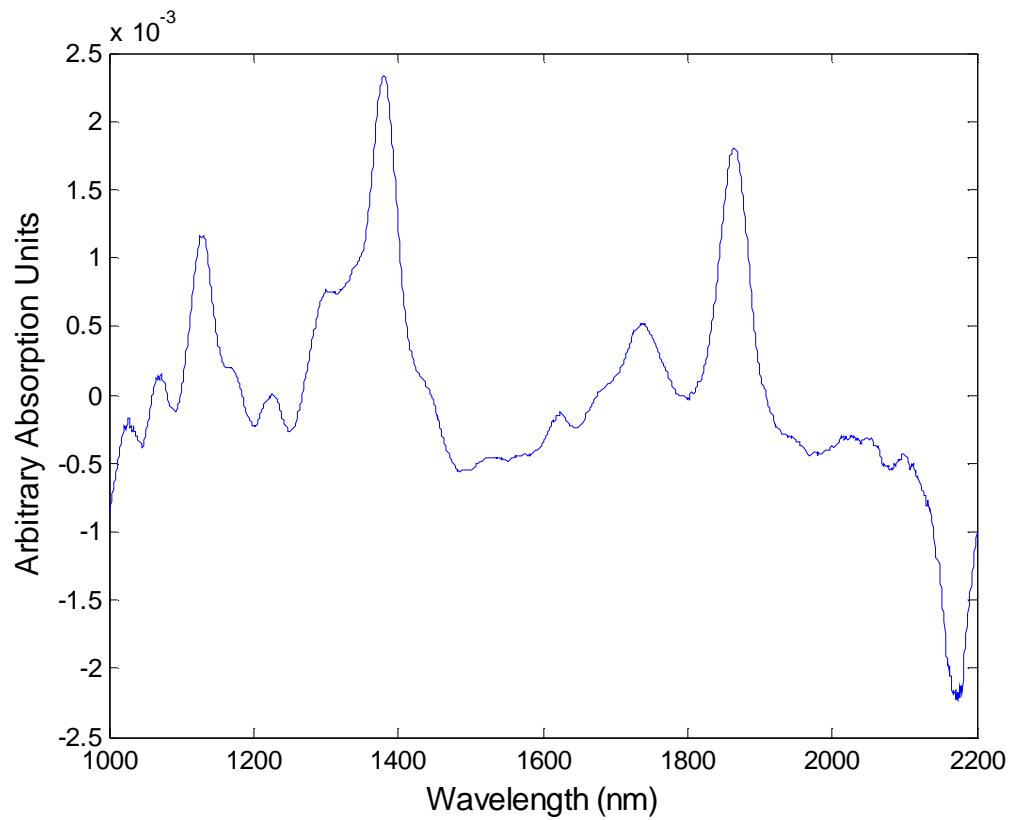


Figure 28: Savitsky-Golay treated spectrum from the LWNIR analyzer.

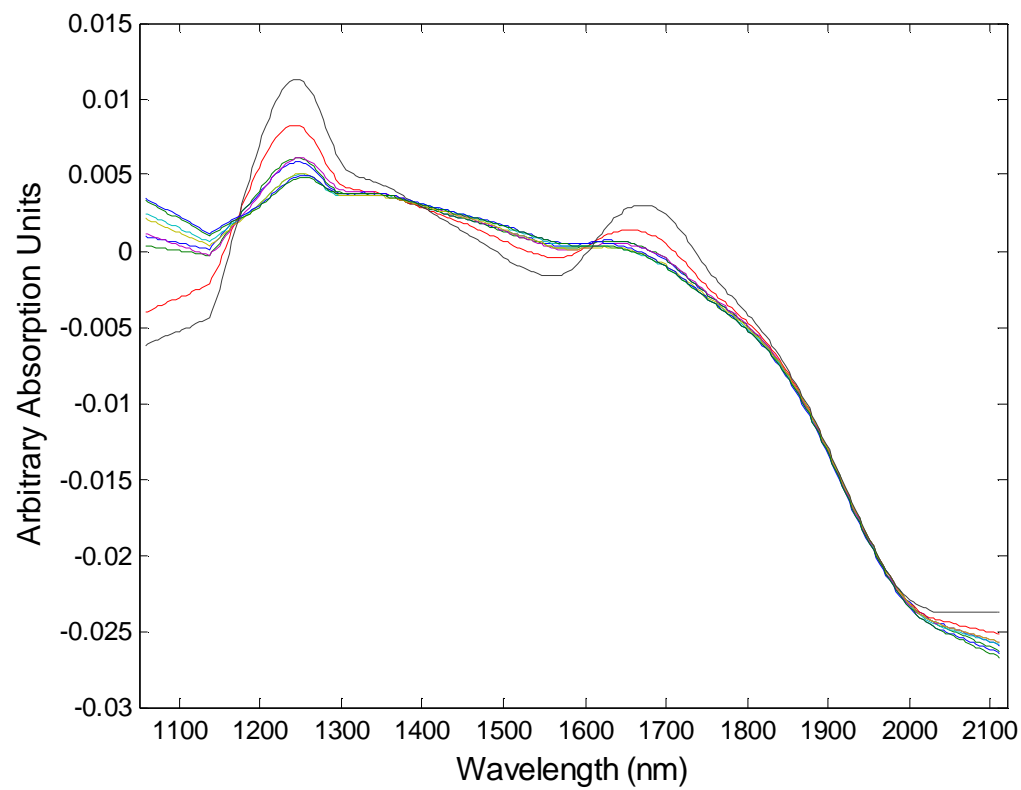


Figure 29: Savitsky-Golay treated spectra from the AOTF-NIR analyzer.

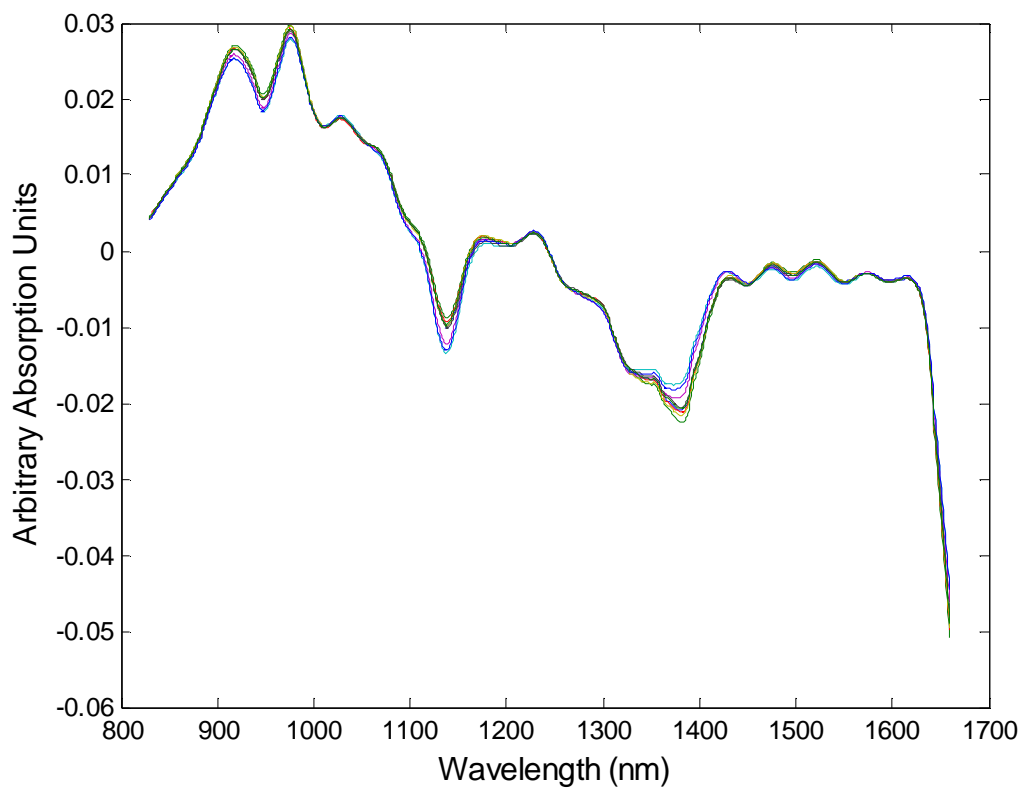


Figure 30: Savitsky-Golay treated spectra from the SWNIR analyzer.

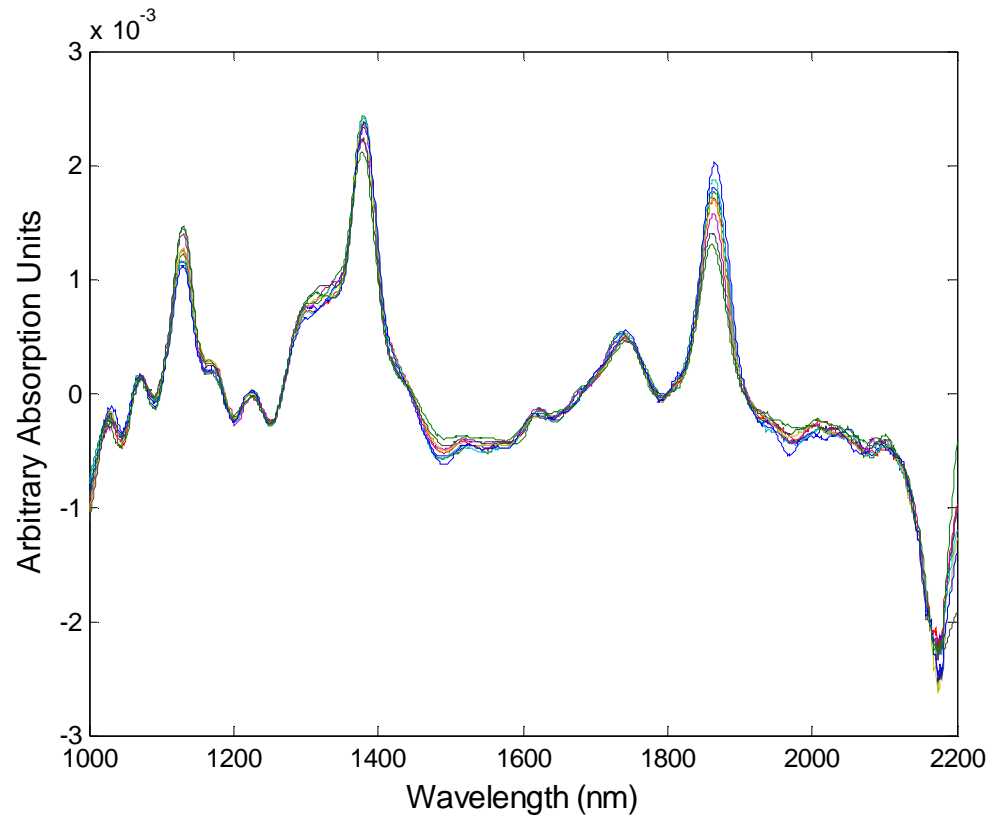


Figure 31: Savitsky-Golay treated spectra from the LWNIR analyzer.

Signal Correction

Several techniques of signal correction were investigated to deal with the inherent difficulties of reflectance spectroscopy. Figure 32 shows raw spectra that have only been DCT filtered. There are three spectra of the same pulp sample that were collected consecutively on the LWNIR spectrometer. The spectra are similar, but show some offset in particular regions. In general, one would expect spectra of the same pulp sample collected on the same analyzer to line up on top of one another. The offsets can most likely be attributed to light scattering effects. Figures 33 and 34 show the same spectra after using standard normal variate scaling (SNV) and multiplicative scatter correction (MSC), respectively. Both SNV and MSC techniques help correct light scattering and have very similar effects on the spectra. There is very little difference between treated spectra of the same sample, which can improve calibration models. Essentially, SNV and MSC decrease spectral variation among samples of the same class.

Orthogonal signal correction (OSC), when applied to the spectra, drastically improved the calibration models, but these models failed to estimate unknown samples accurately. Figures 35 and 36 show differentiated spectra of all samples from set C, collected on the LWNIR analyzer before and after OSC was applied. Figures 37 and 38 show spectra for three samples with kappa number values of 18, 41, and 85 before and after OSC was applied. There are three spectra for each sample. In these figures it is clear that OSC aligns spectra of the same sample class and creates good separation between samples with different measured values. OSC uses the measured values as a parameter to create a set of weights to correct the spectra. Calibration models created using OSC should certainly have good correlations, because the spectra are adjusted

according to the measured values of the pulp samples. For estimating values for the unknown samples, the weights created from the calibration model are applied to new spectra of the unknowns. With the samples tested the parameters created with OSC did not prove to properly correct the new spectra of unknowns. This indicates that spectral differences determined through OSC are neither universal nor applicable to data outside of the calibration set, for the data analyzed in this research.

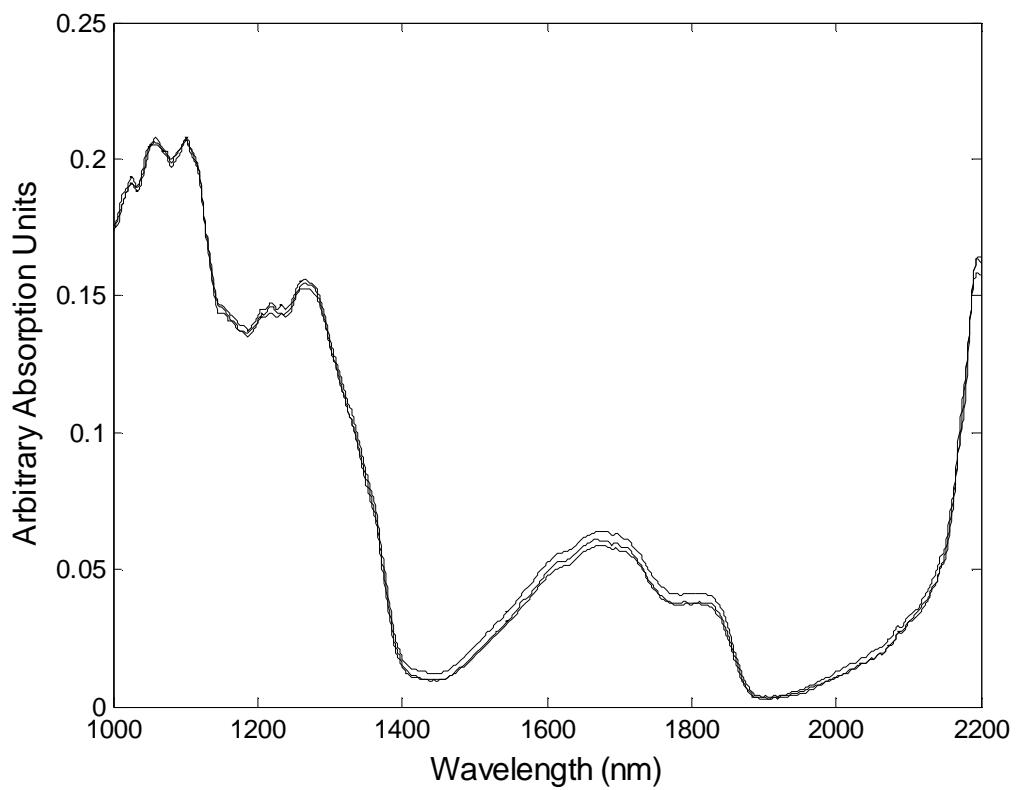


Figure 32: DCT filtered spectra of one sample.

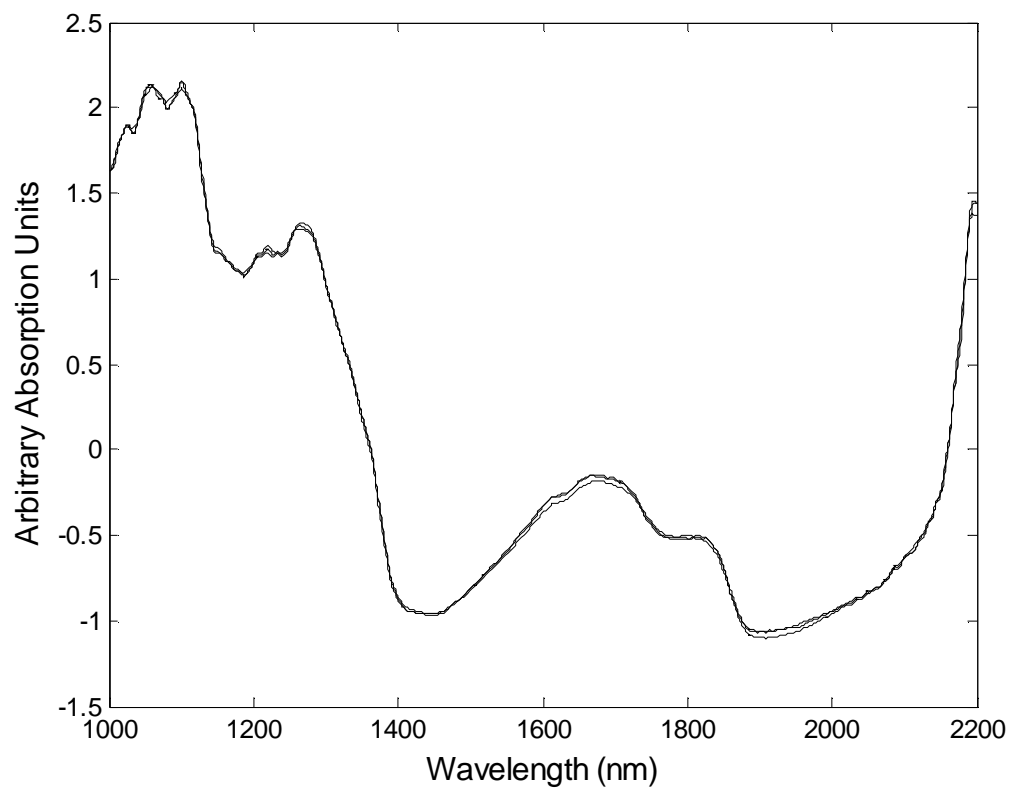


Figure 33: Figure 32 spectra with SNV applied.

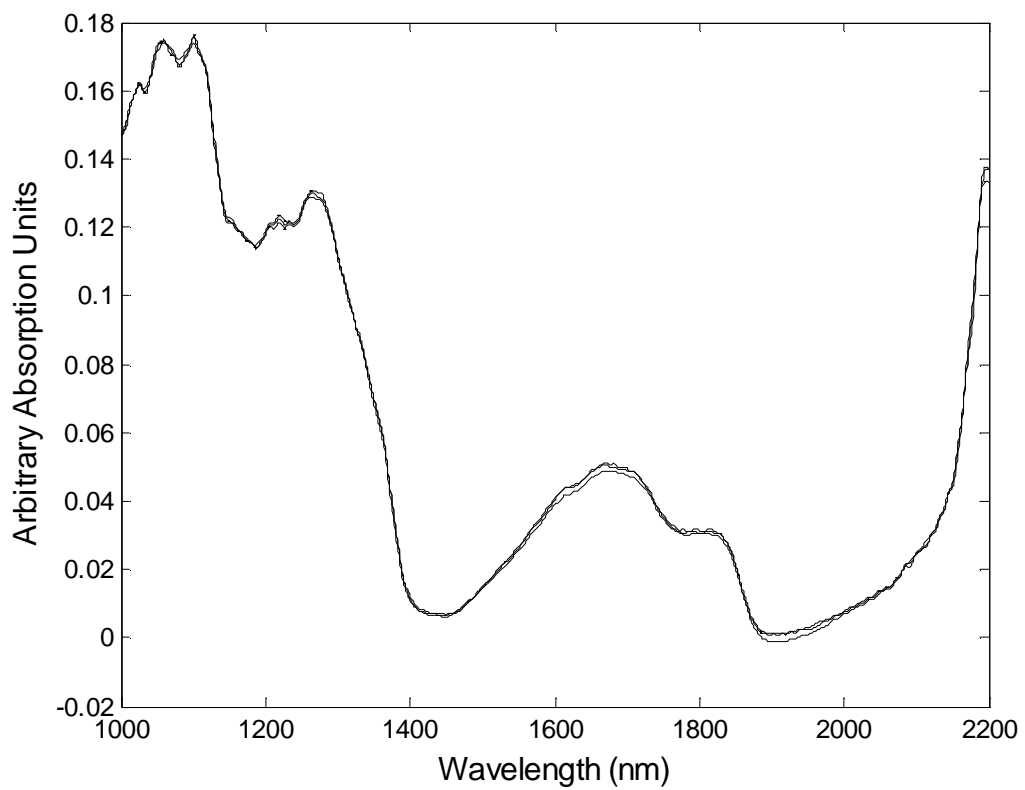


Figure 34: Figure 32 spectra with MSC applied.

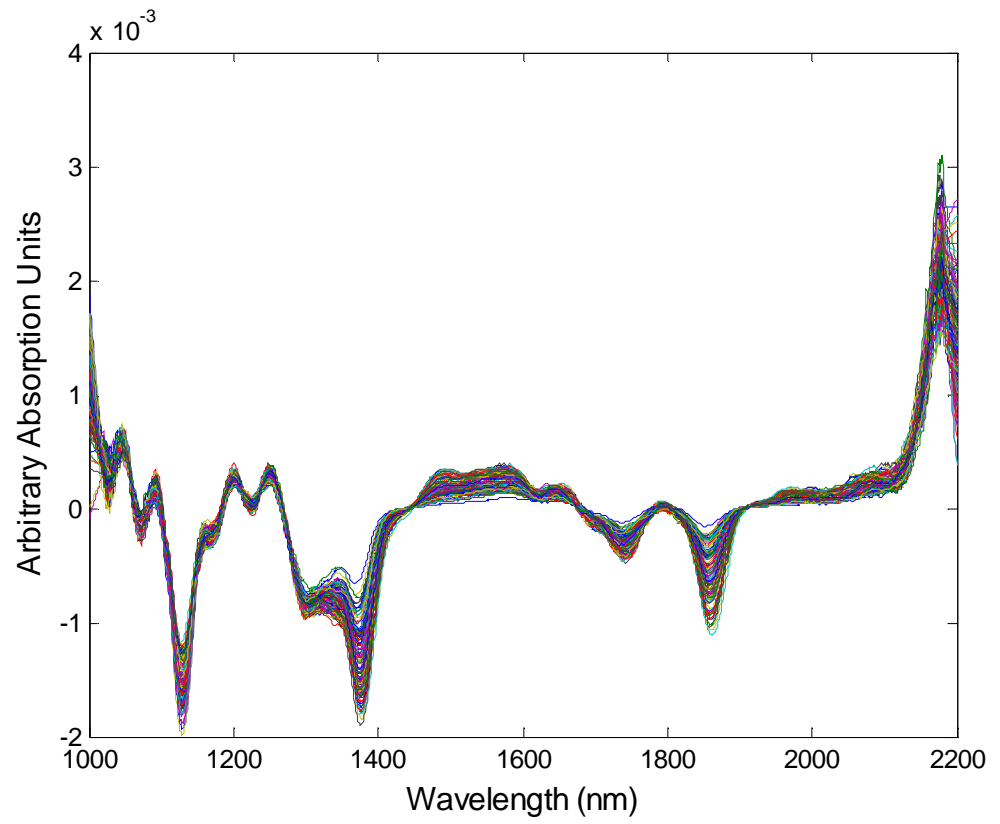


Figure 35: Savitsky-Golay treated spectra from LWNIR analyzer.

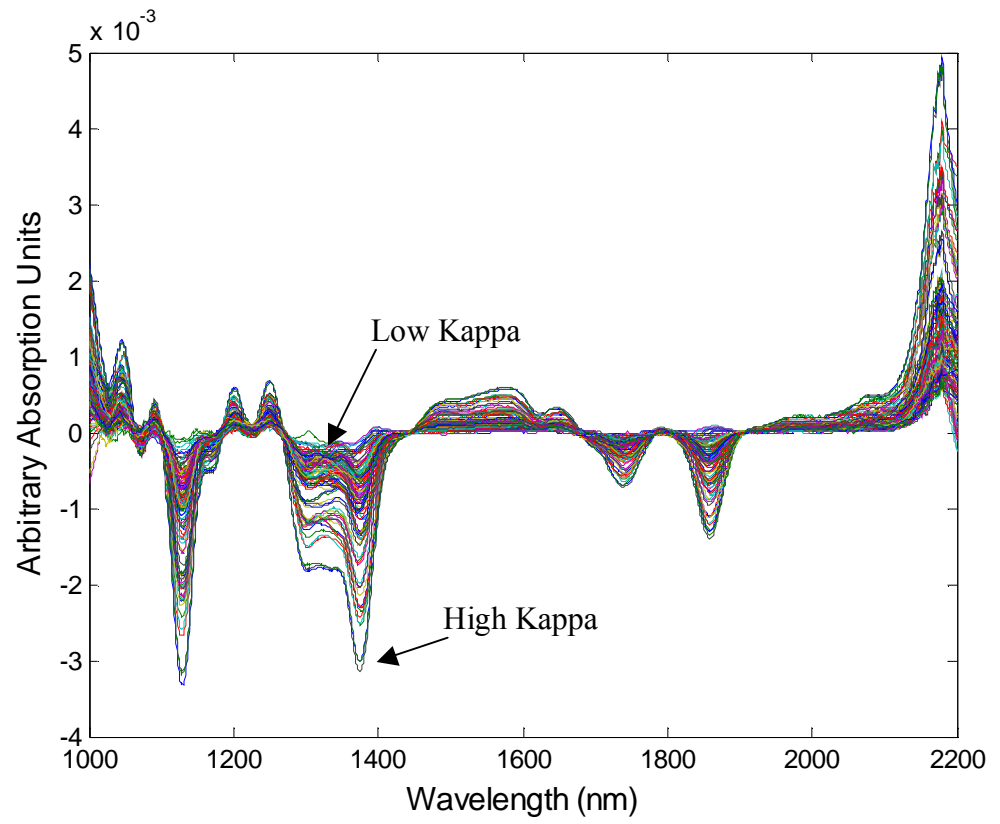


Figure 36: Previous spectra with OSC applied.

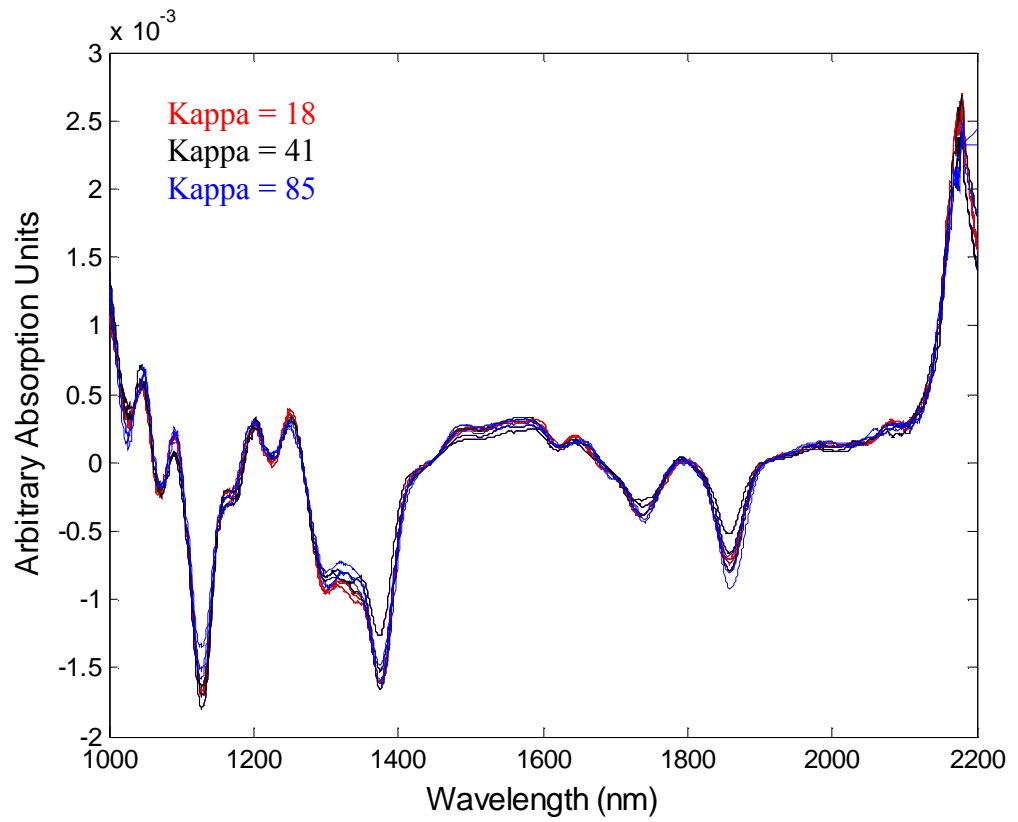


Figure 37: Three samples with widely varying kappa number.

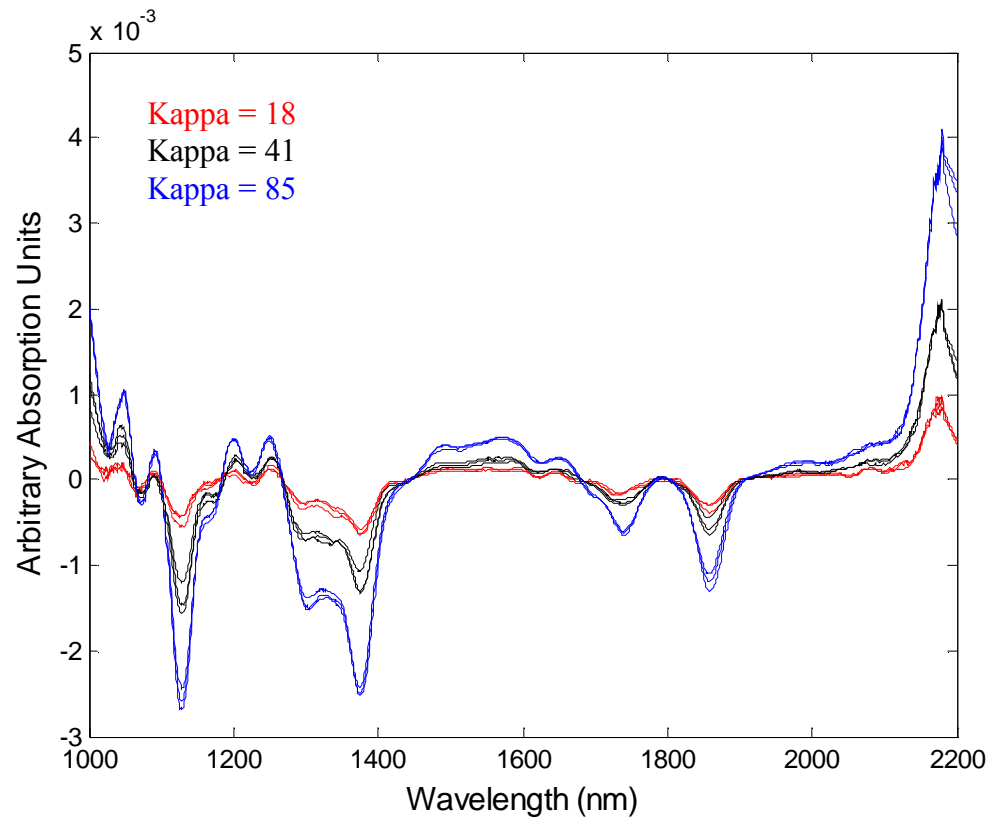


Figure 38: Previous spectra treated with OSC.

Pulp Calibration Models and Predictions

All of the aforementioned data treatments have been utilized considerably throughout the development of calibration models for kappa and yield prediction. Numerous combinations and manipulations of these techniques have been employed with all of the sample sets and spectra collected from the different spectrometers. The application of these techniques has led to improvements in the calibration plots and the ability to accurately predict kappa numbers of some mill samples.

Calibration models developed using pulp sample set C in conjunction with the LWNIR prototype spectrometer have shown the best ability to predict samples that are in the model, but failed to predict unknown lab generated samples. These poor prediction plots had R^2 values of 0.5 or less, which shows essentially no correlation. However, the calibration plots showed good correlations with eight loadings in the PLS regression model. These calibration plots were produced using only Kubelka-Munk linearization along with multiplicative scatter correction (MSC). Figures 39 and 40 show the calibration plots for kappa and yield, respectively. The plots show the actual measured values as the independent variable and the values predicted by the calibration models as the dependent variable.

Since the prediction of unknown lab samples was poor, a technique was employed to determine repeatability of spectral measurements. Three scans of each sample were taken consecutively, only repositioning the sample each time. Calibrations were then built with two spectra from each sample and the third set of spectra was used for prediction. With this approach reasonable predictions were achieved. However, spectra of the samples used in the prediction set were built into the calibration. Obviously this is

not a good indicator of the ability of the model to predict unknowns. Figure 41 and 42 show the aforementioned prediction plots for kappa and yield, respectively. It is clear that correlations of these plots are not as good as the calibration plots. This would suggest that the variability in the packing and surface of the pulp pads has a considerable effect on the resultant spectra. This is most likely due to the orientation of the reflectance set-up. Although many attempts have been made to optimize the components, a successful iteration of design has not yet been reached. The collected light is most likely only the specular reflectance or that which is reflected off of the surface of the pulp rather than light that has penetrated the pulp pad. A better raw spectrum is essential for the development of useful calibration models.

A calibration model using lab pulp samples was built to estimate a set of unknown mill pulp samples of kappa number ranging from 14 to 34. The model was built with sample set C and used Kubelka-Munk linearization, DCT filtering, and Savitsky-Golay differentiation for the spectral pretreatments. This calibration model predicted the unknown kappa values of the mill samples fairly well using eight loadings with the PLS regression. Table 1 shows the actual and predicted values for the mill samples. The model estimated each sample value within two kappa numbers of their actual value. Figure 43 shows the plot for the calibration model and figure 44 shows the actual prediction curve for the mill samples. The results are good considering the model was fairly accurate for samples from six different mills. In practice, calibrations models will most likely be tailored for a particular mill to provide the most robust predictions.

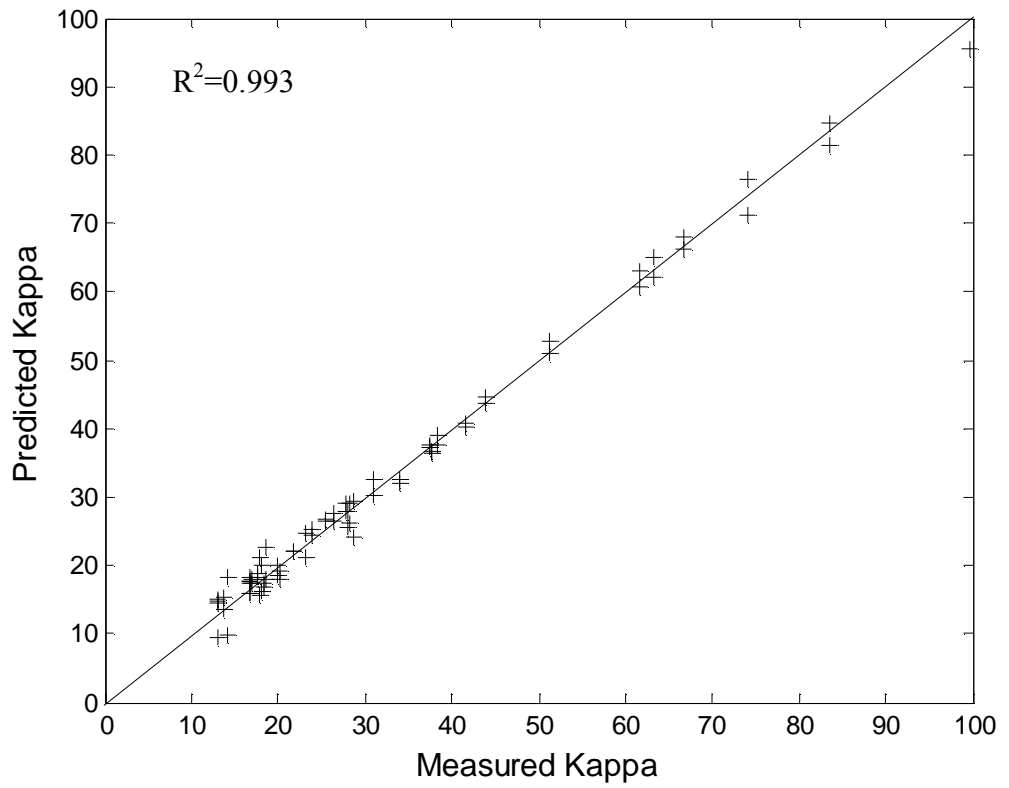


Figure 39: Calibration curves for kappa measurement.

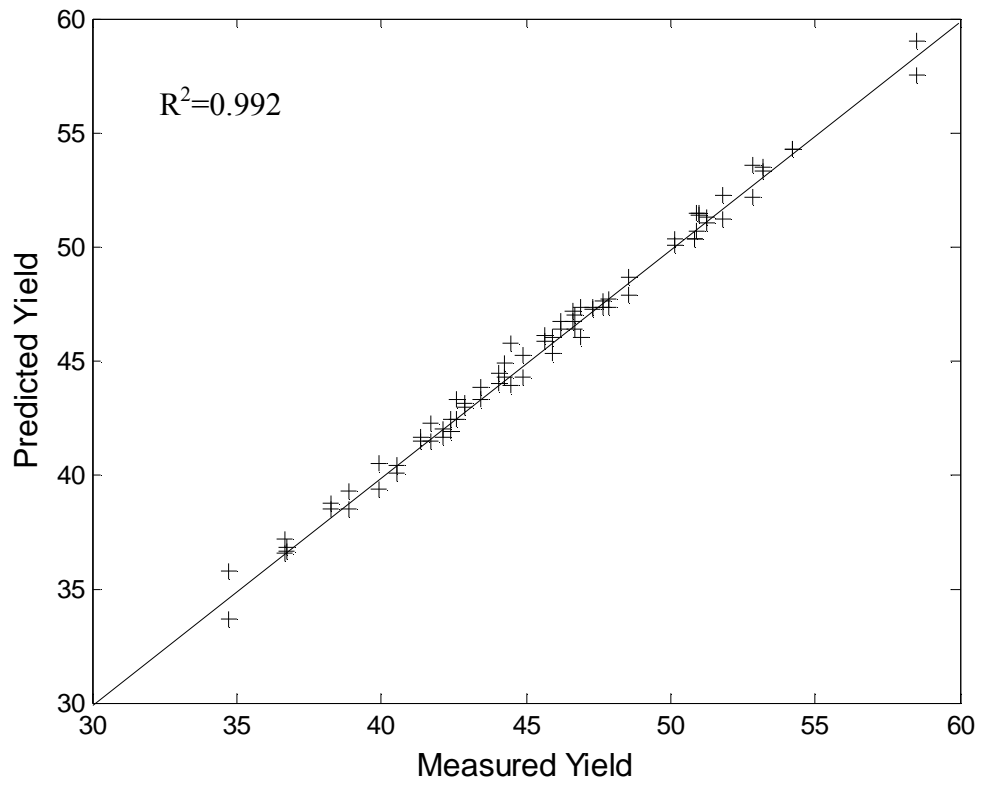


Figure 40: Calibration curve for yield measurement.

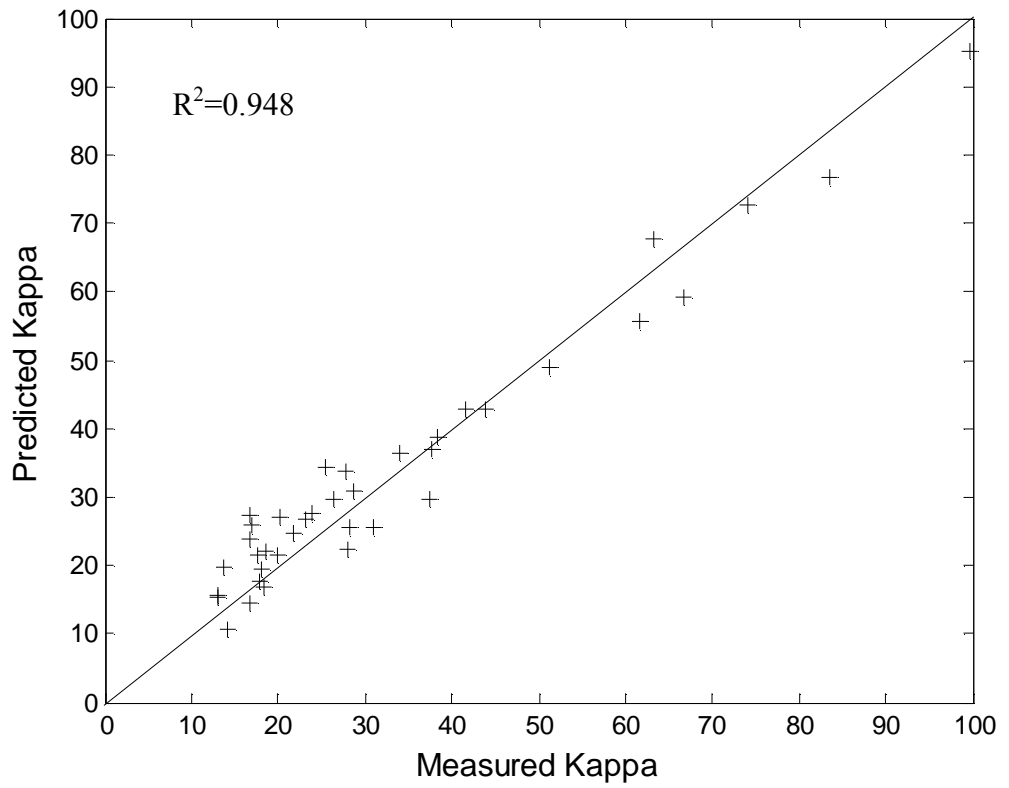


Figure 41: Prediction curve for kappa measurement.

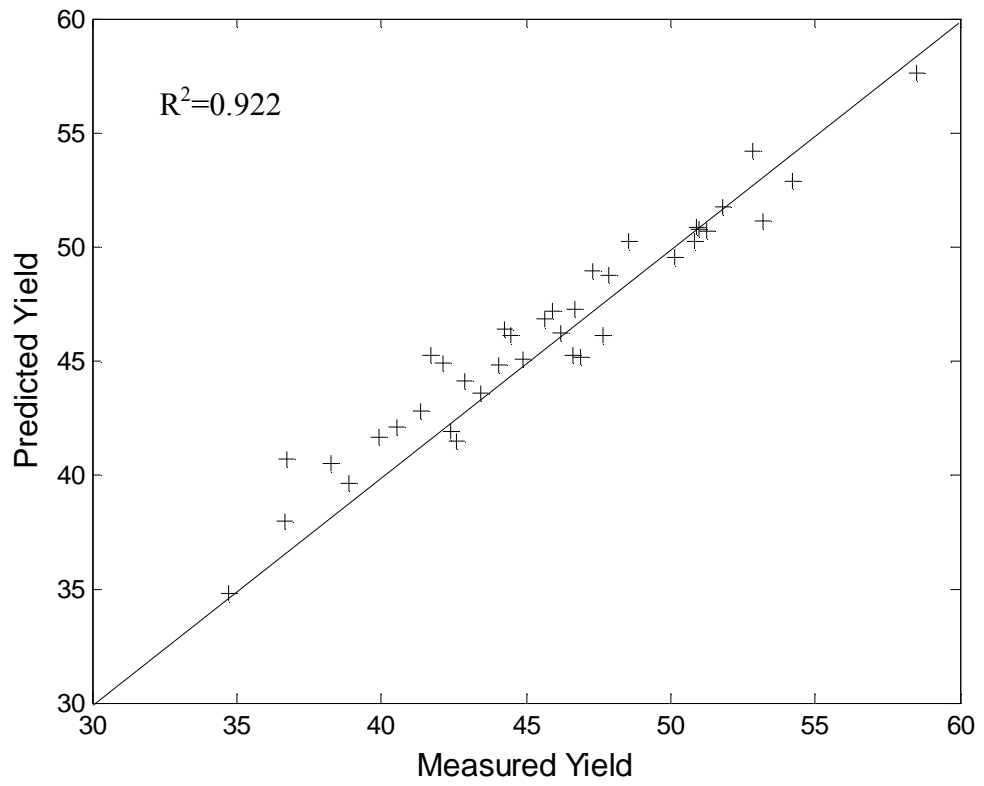


Figure 42: Prediction curve for yield measurement.

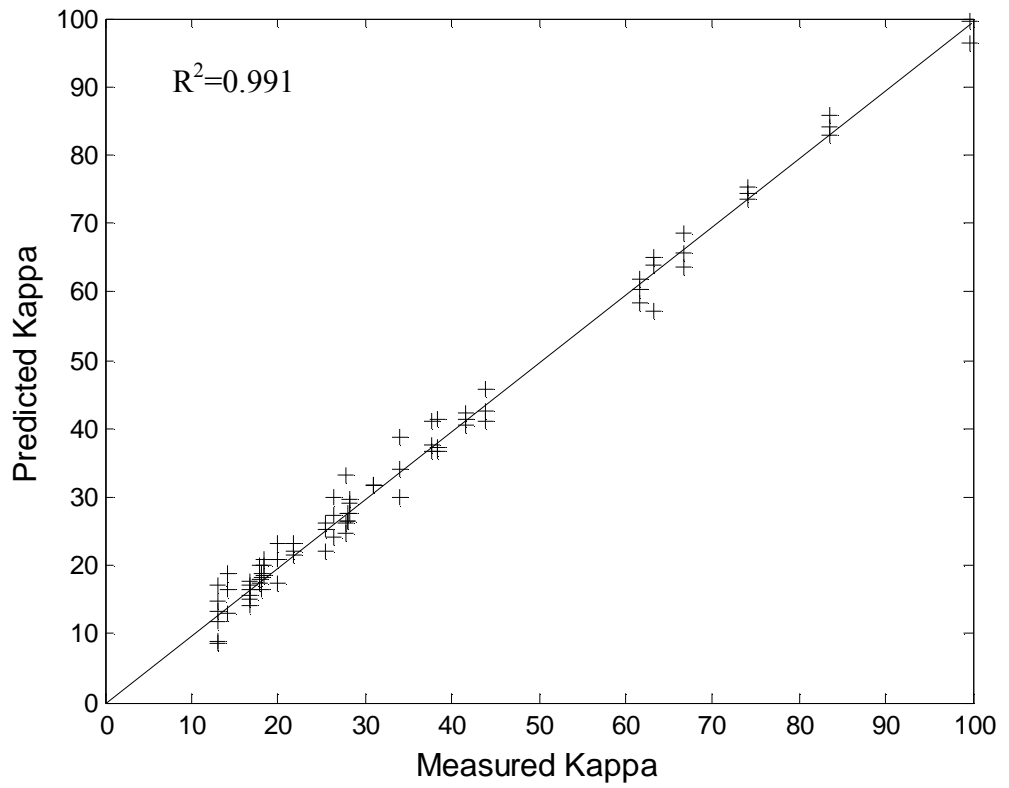


Figure 43: Calibration curve for kappa measurement of mill samples.

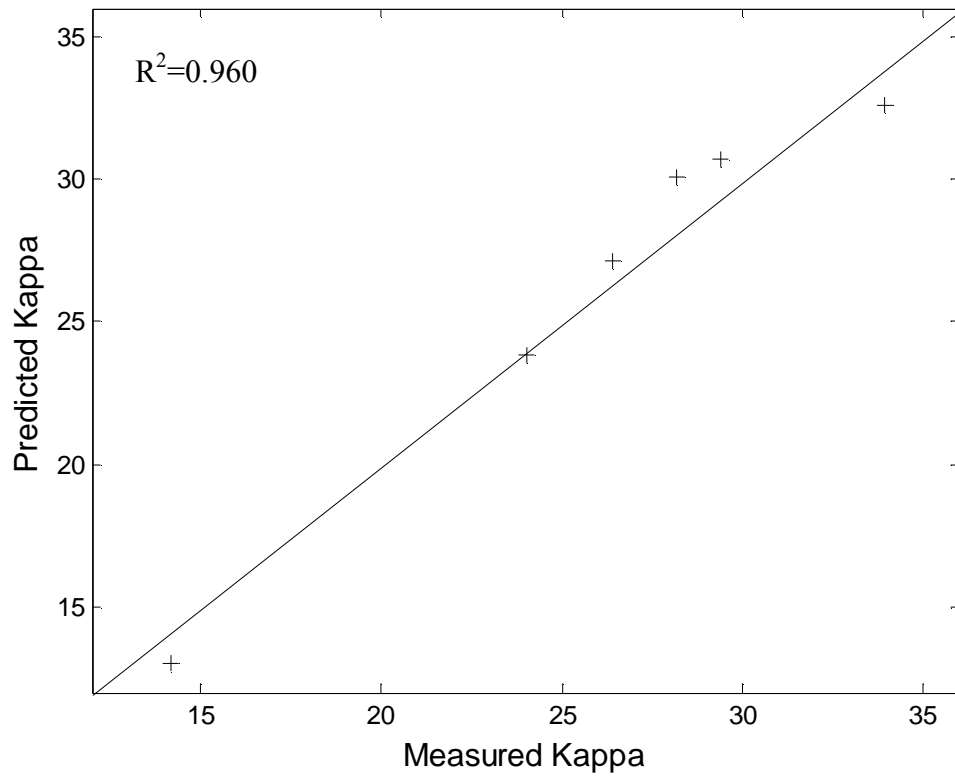


Figure 44: Prediction curve for kappa measurement of mill samples.

Mill Sample	Predicted Kappa	Actual Kappa	Kappa Difference
A	30.1	28.2	+1.9
B	13.0	14.2	-1.2
C	32.6	33.9	-1.3
D	27.1	26.4	+0.7
E	23.8	24.0	-0.2
F	30.7	29.4	+1.3

Table 1: Actual and predicted values for mill samples.

Black Liquor Calibration Models and Predictions

Only minor investigations were made into the ability to predict yield and kappa number using spent black liquor spectra. A limited set of black liquor from sample set B was available for analysis. Only concentrated black liquor was considered for the calibration. The diluted black liquor was at too low a concentration and only appeared as water when the spectra were analyzed.

Figure 45 shows typical concentrated black liquor spectra for a high and low kappa and yield value. Collecting spectra of the liquor allowed for good light throughput and fairly clean and defined spectra were achieved. No data pretreatment was necessary for building the calibration model. Figures 46 and 47 show the calibration plots for the black liquor spectra. Figures 48 and 49 show the prediction plots for the black liquor. The calibration model predicted both pulp yield and kappa number with some accuracy.

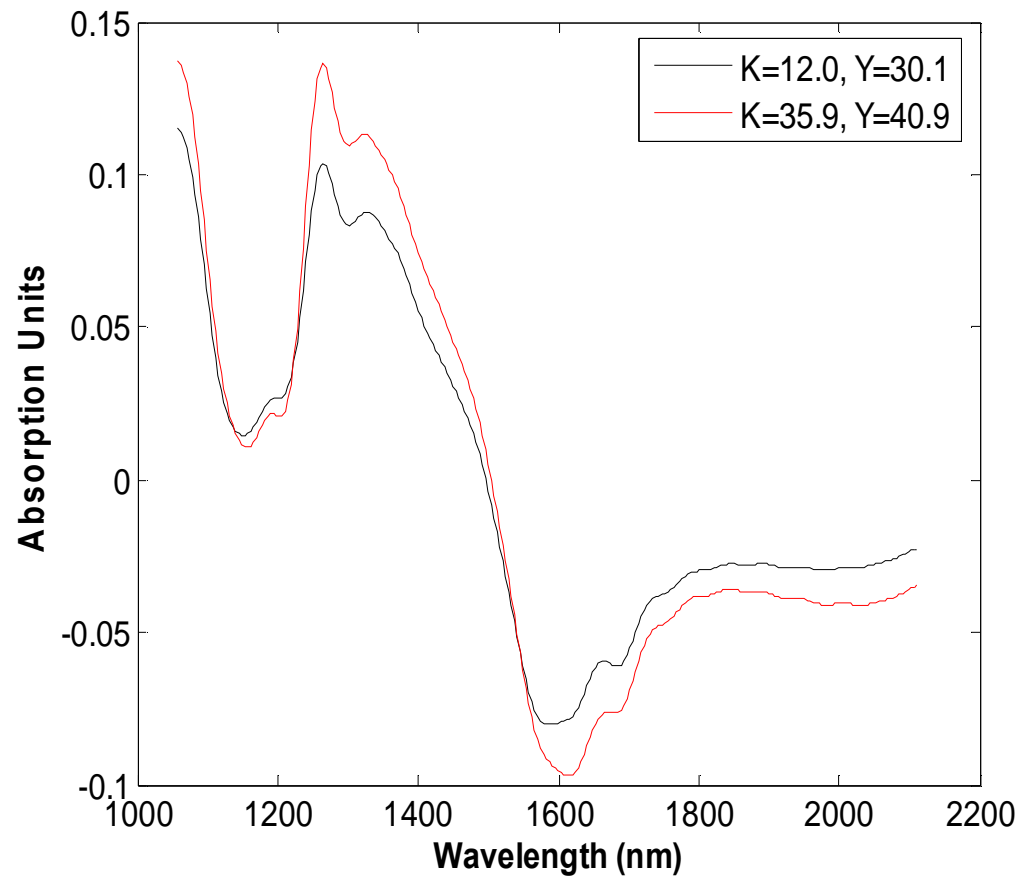


Figure 45: Typical spectra for spent black liquor.

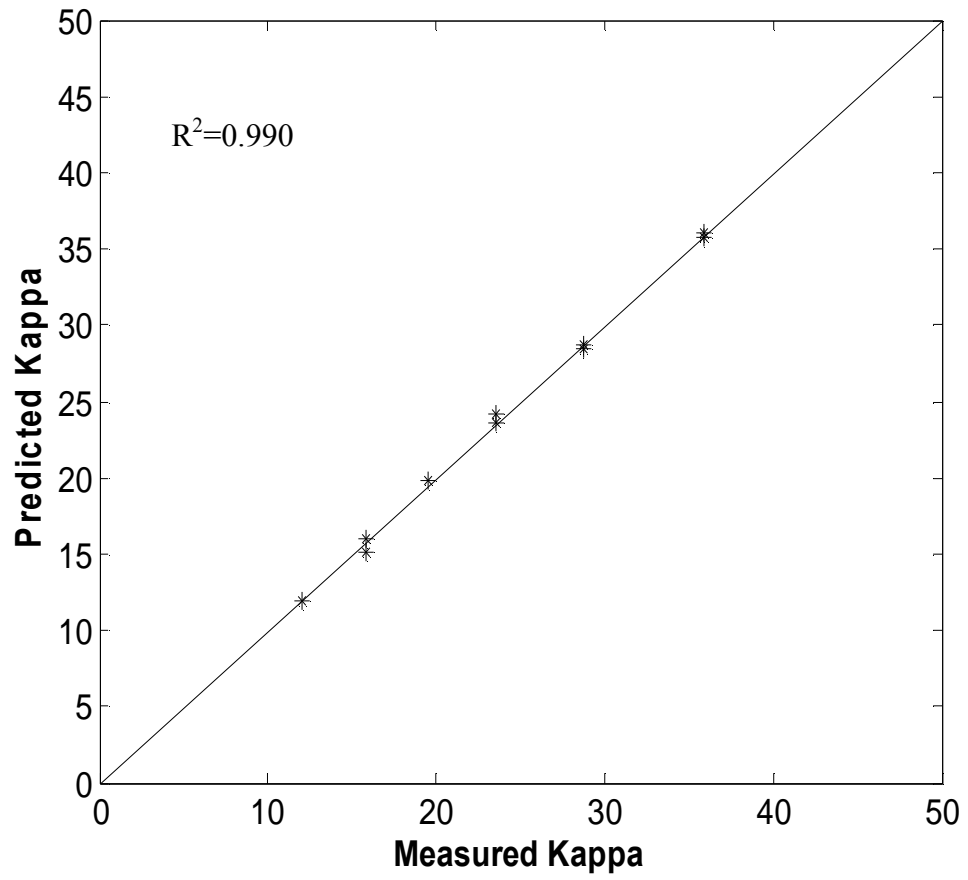


Figure 46: Black liquor calibration curve for kappa measurement.

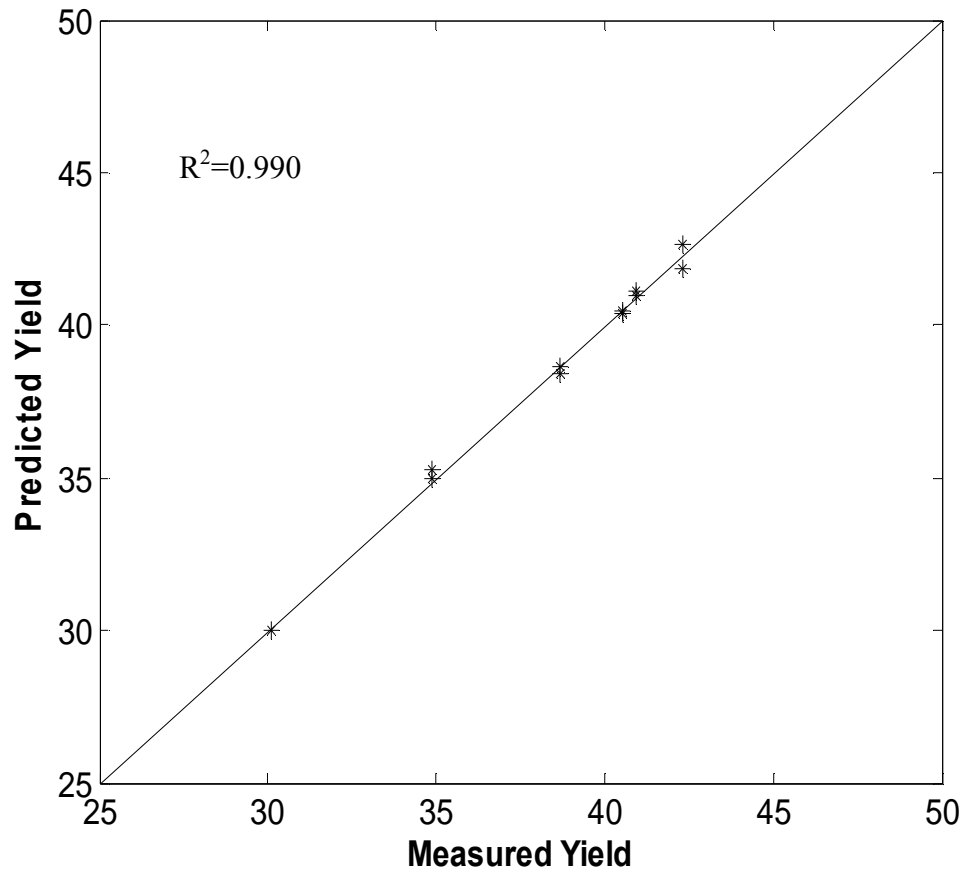


Figure 47: Black liquor calibration curve for yield measurement.

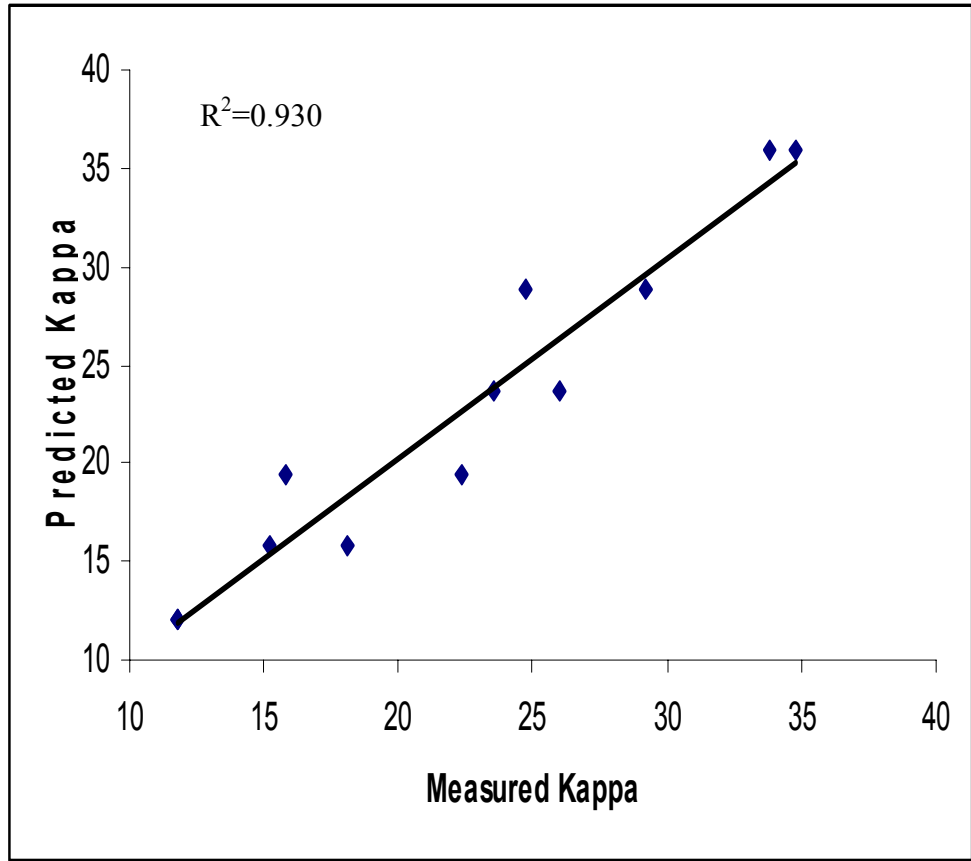


Figure 48: Black liquor prediction curve for kappa measurement.

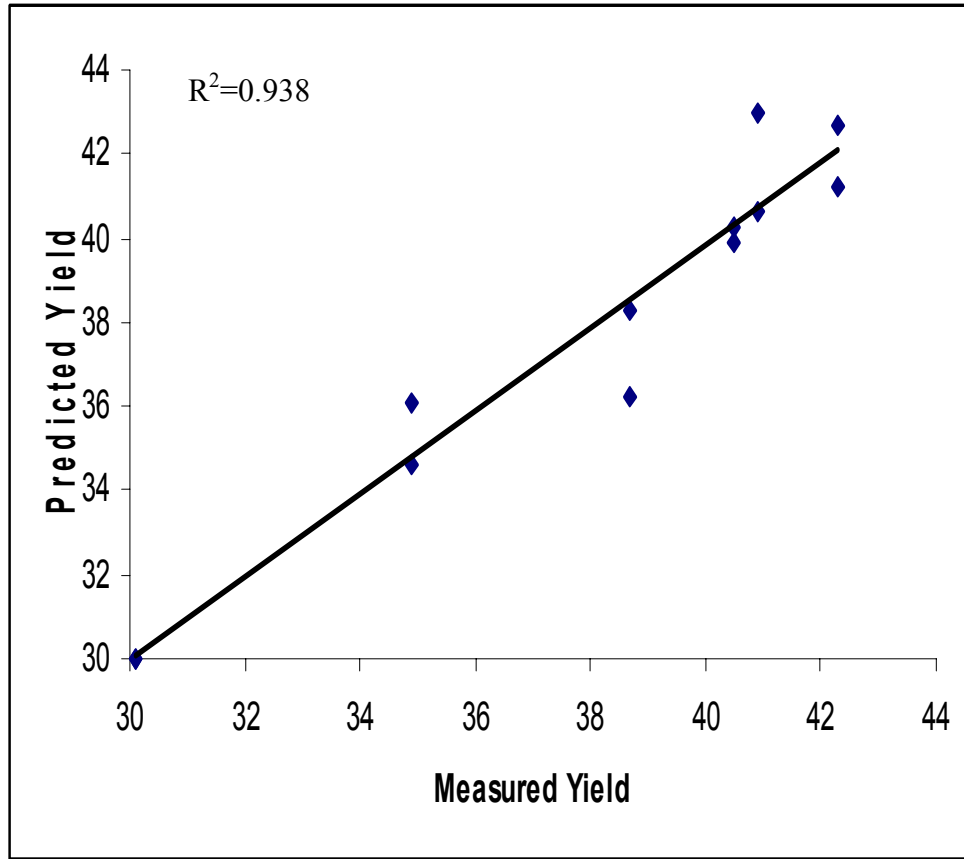


Figure 49: Black liquor prediction curve for yield measurement.

CONCLUSIONS

The ultimate goal of this research was to build robust calibration models for the prediction of kappa and yield values for unknown samples. Techniques for collecting the black liquor transmission spectra were straight forward and the development of good calibration models required few iterations. Kappa and yield values of unknown black liquor samples were estimated with good accuracy using the calibration models.

Correlations relating pulp reflectance data with yield and kappa values was not as easily realized. Building such calibration models required optimizations of the spectrometer, sample presentation, and spectral preprocessing techniques. Spectral features relating to pulp properties (e.g. kappa, yield, etc.) are quite subtle and require more advanced spectral processing techniques to extract as compared to transmission methods. The key to building models that predict unknowns accurately lies in maximizing the signal to noise ratio of the spectra and determining the correct configuration for the reflectance apparatus.

Several reflectance arrangements are available, but this research was concerned with using an arrangement that would lend itself well to reliable and simple online and lab based implementation in the mill environment. Previous work from researchers in this field used sophisticated lab based reflectance arrangements (e.g. integrating spheres)

and tedious pulp sample pre-treatments, however, these methods cannot be easily implemented in a non-idealized mill environment.

Despite the difficulties involved, a calibration model was created that accurately predicted the kappa values for six different mill pulp samples. This result is very promising, because in practice calibrations will most likely be tailored for a specific mill. Eventual calibrations built for online control will certainly be more robust due to their specificity.

BIBLIOGRAPHY

1. Smook, G.A., "Handbook for pulp and paper technologists", Tappi Press, Atlanta, 1992
2. Hodges, R.E., "Applications of near infrared spectroscopy in the pulp and paper industry", Auburn University Press, Auburn, AL, 1999
3. Grace, T.M. and Malcolm, E.W., (ed.) "Pulp and paper manufacture, Vol. 5, Alkaline pulping", Tappi Press, Atlanta, 1989
4. Tappi Test Methods T 236 cm – 85 (1985)
5. Kubulnieks, E., Lundqvist, S.O. and Pettersson, T. – *Tappi J* **70**(11):38(1987)
6. Wallbacks, L., Edlund, U. and Norden, B. – *Tappi J* **74**(10):201(1991)
7. Schultz, T.P. and Burns, D.A. – *Tappi J* **73**(5):209(1990)
8. Bjarnestad, S. and Dahlman, O. - *Anal. Chem.* **74**(22):5851(2002)
9. Bhardwaj, N.K., Hoang, V. and Nguyen, K.L. – *Carbohydrate Polymers* **61**:5(2005)
10. Birkett, M.D. and Gambino, M.J.T. – *Tappi J* **72**(9):193(1989)
11. Fardim, P., Ferreira, M.M.C. and Duran, N. – *J Wood Chem. And Tech.* **22**(1):67(2002)
12. Wright, J.A., Birkett, M.D. and Gambino, M.J.T. - *Tappi J* **73**(8):164(1990)
13. Michell, A.J. – *Appita* **48**(6):425(1995)

14. Woitkovich, C.P., McDonough, T. J. and Malcolm, E.W. *Tappi Pulping Conference Proceedings* (1994):721
15. Hodges, R.E. and Krishnagopalan, G.A. – *Tappi J* **82**(9):101(1999)
16. Smith, S., “Infrared spectral interpretation”, CRC Press, New York, 1999
17. Workman, J. and Springsteen, A., “Applied Spectroscopy”, Academic Press, New York, 1998
18. Baillet, A., Chaminade, P. and Ferrier, D. – *Analisis Magazine* **26**(4):33(1998)
19. Despagne, F., Estienne, F. and Massart, D.L. - *Chemometrics and Intelligent Laboratory Systems* **73**:207(2004)
20. Tobias, R.D. – “An introduction to partial least squares regression” SAS Institute Inc., Cary, NC
21. Esteban-Diez, I., Gonzalez-Saiz, J.M. and Jose-Nistal, A. – *Analytica Chimica Acta* **509**:217(2004)
22. Gunzler, H. and Hans-Ulrich, G., “IR spectroscopy”, Wiley-VCH, Weinheim, Germany, 2002

APPENDIX A
PULP SAMPLE DATA

Sample Set A (samples 1-32)

Run #	Cook Time (h)	Cook Temp. (C)	EA (g/L as Na ₂ O)	Yield	Kappa
1	1	160	36.9	61.4	74.2
2	1	160	42.2	60.8	66.7
3	1	160	51.3	56.8	58.6
4	1	160	57.0	52.7	51.4
5	1	160	63.8	54.1	41.3
6	1	160	71.6	53.1	35.1
7	1	160	76.7	50.0	33.1
8	1	160	84.0	48.3	32.4
9	1	165	36.9	54.6	39.9
10	1	165	42.2	50.0	32.6
11	1	165	51.3	46.4	30.0
12	1	165	57.0	45.1	26.4
13	1	165	63.8	46.0	25.5
14	1	165	71.6	45.2	26.8
15	1	165	76.7	42.3	22.3
16	1	165	84.0	40.6	21.9
17	1	170	36.9	52.0	34.3
18	1	170	42.2	48.6	30.7
19	1	170	51.3	45.1	23.7
20	1	170	57.0	44.0	23.4
21	1	170	63.8	42.5	21.0
22	1	170	71.6	41.8	20.4
23	1	170	76.7	38.5	19.9
24	1	170	84.0	36.6	16.4
25	1	175	36.9	49.0	31.7
26	1	175	42.2	45.9	26.1
27	1	175	51.3	43.1	22.3
28	1	175	57.0	41.6	21.6
29	1	175	63.8	39.1	19.2
30	1	175	71.6	37.8	18.6
31	1	175	76.7	35.3	17.0
32	1	175	84.0	34.6	16.2

Sample Set A (samples 33-80)

Run #	Cook Time (h)	Cook Temp. (C)	EA (g/L as Na ₂ O)	Yield	Kappa
33	1.5	165	36.9	53.5	33.1
34	1.5	165	42.2	47.5	30.3
35	1.5	165	51.3	46.4	27.0
36	1.5	165	57.0	44.9	26.4
37	1.5	165	63.8	43.2	24.7
38	1.5	165	71.6	44.4	26.2
39	1.5	165	76.7	35.6	18.8
40	1.5	165	84.0	33.0	14.6
41	1.5	170	36.9	44.6	28.1
42	1.5	170	42.2	47.6	30.1
43	1.5	170	51.3	44.7	26.7
44	1.5	170	57.0	42.3	23.7
45	1.5	170	63.8	41.3	18.9
46	1.5	170	71.6	40.9	18.2
47	1.5	170	76.7	36.1	14.2
48	1.5	170	84.0	36.5	16.1
49	1.5	160	36.9	59.9	39.9
50	1.5	160	42.2	53.5	35.5
51	1.5	160	51.3	47.8	30.0
52	1.5	160	57.0	49.0	29.1
53	1.5	160	63.8	47.5	29.2
54	1.5	160	71.6	46.2	27.8
55	1.5	160	76.7	43.2	22.4
56	1.5	160	84.0	42.7	23.0
57	2	160	36.9	62.4	46.4
58	2	160	42.2	52.1	36.3
59	2	160	51.3	47.4	28.1
60	2	160	57.0	45.5	24.0
61	2	160	63.8	43.1	22.9
62	2	160	71.6	42.8	22.9
63	2	160	76.7	41.5	21.5
64	2	160	84.0	39.8	20.0
65	2	165	36.9	55.6	36.3
66	2	165	42.2	48.7	29.2
67	2	165	51.3	45.4	26.5
68	2	165	57.0	44.3	24.5
69	2	165	63.8	41.8	21.5
70	2	165	71.6	40.3	20.8
71	2	165	76.7	38.7	19.8
72	2	165	84.0	37.9	18.4
73	2	170	36.9	49.2	29.9
74	2	170	42.2	46.4	27.0
75	2	170	51.3	45.9	27.1
76	2	170	57.0	43.6	22.5
77	2	170	63.8	41.3	22.1
78	2	170	71.6	39.2	19.1
79	2	170	76.7	38.6	19.7
80	2	170	84.0	36.7	18.1

Sample Set B

Run #	Cook Time (h)	Cook Temp. (C)	EA (g/L as Na ₂ O)	Yield	Kappa
1	1.5	170	68.5	36.8	21.0
2	1.5	170	80.4	34.6	17.8
3	1.5	170	76.5	37.7	15.7
4	1.5	170	72.4	35.1	14.3
5	1.5	170	89.6	32.7	12.7
6	1.5	170	82.5	34.0	14.4
7	1.5	170	87.5	32.4	12.5
8	1.5	170	93.5	30.1	13.0
9	2	170	90.2	34.9	15.8
10	2	170	100.2	32.2	18.2
11	2	170	106.8	31.8	21.1
12	2	170	114.1	28.2	17.0
13	1	170	90.2	37.5	22.7
14	1	170	100.2	35.0	19.4
15	1	170	106.8	35.9	28.0
16	1	170	114.1	34.3	24.0
17	1.5	170	90.2	35.1	15.0
18	1.5	170	100.2	32.6	17.2
19	1.5	170	106.8	32.9	21.1
20	1.5	170	114.1	31.1	18.4
21	0.5	170	90.2	40.2	29.8
22	0.5	170	100.2	37.1	24.5
23	0.5	170	106.8	39.2	39.4
24	0.5	170	114.1	37.8	40.6
25	2	160	90.2	40.5	24.2
26	2	160	100.2	38.7	20.0
27	2	160	106.8	40.9	35.9
28	2	160	114.1	39.7	33.8
29	1	160	90.2	42.3	27.3
30	1	160	100.2	40.5	27.5
31	1	160	106.8	43.7	55.4
32	1	160	114.1	42.9	57.6
33	1.5	160	90.2	42.5	26.5
34	1.5	160	100.2	39.7	23.3
35	1.5	160	106.8	43.2	41.0
36	1.5	160	114.1	41.0	53.2

Sample Set C

Run #	Cook Time (h)	Cook Temp. (C)	EA (g/L as Na ₂ O)	Yield	Kappa
1	1	170	90.0	39.9	18.2
2	1	170	60.0	45.9	41.7
3	1	170	30.0	56.7	13.7
4	1.5	170	90.0	36.7	31.1
5	1.5	170	60.0	42.6	38.5
6	1.5	170	30.0	51.0	83.5
7	0.5	170	90.0	44.1	27.8
8	0.5	170	60.0	51.8	74.1
9	0.5	170	30.0	54.6	16.7
10	0.5	170	90.0	42.9	20.0
11	0.5	170	60.0	50.9	16.7
12	0.5	170	30.0	60.4	20.2
13	2.5	170	90.0	36.8	14.2
14	2.5	170	60.0	44.9	17.9
15	2.5	170	30.0	48.7	26.4
16	2	170	90.0	38.8	28.2
17	2	170	60.0	42.1	99.8
18	2	170	30.0	57.6	18.3
19	3	170	90.0	34.7	17.9
20	3	170	60.0	41.4	63.3
21	3	170	30.0	51.3	17.0
22	1	170	80.0	46.2	18.6
23	1	170	70.0	46.9	61.6
24	1	170	50.0	58.5	13.1
25	1.5	170	80.0	42.4	13.0
26	1.5	170	70.0	43.5	52.5
27	1.5	170	50.0	52.9	37.7
28	2	170	80.0	41.7	66.7
29	2	170	70.0	44.5	28.0
30	2	170	50.0	53.2	25.6
31	2.5	170	80.0	38.3	44.0
32	2.5	170	70.0	40.6	23.8
33	2.5	170	50.0	51.0	37.5
34	2.5	160	90.0	47.9	28.6
35	2.5	160	60.0	54.2	21.8
36	2.5	160	80.0	47.7	33.8
37	3	160	90.0	44.3	23.1
38	3	160	60.0	50.2	16.6
39	3	160	70.0	46.6	18.8
40	2.5	165	40.0	51.2	14.6
41	2.5	165	50.0	48.6	28.1
42	2.5	165	60.0	46.7	30.1
43	3	165	40.0	50.8	26.7
44	3	165	50.0	43.2	23.7
45	3	165	60.0	41.9	18.9

APPENDIX B

MATLAB M.FILES

Data Reorganization: Reorganizes text files of spectra from the NIR analyzer into MxN matrices of wavelength and absorbance values.

```
% rcdatreorg.m

function datmtx = rcdatreorg(a,N,nscans,br,ss,er)

% a = ASCII data matrix originally exported from Black Box program
% datmtx = new ASCII data matrix reorganized into spts x (nscans*N+1)
matrix
% N = number of samples
% nscans = number of scans pers sample (usually 9)
% br = begining point of wavelength range
% ss = step size (wavelength sample increment)
% er = end point of wavelength range

spts = length(br:ss:er); % spts = number of sample points
[ra,ca] = size(a); % ra = number of rows of a, ca = number of columns
of a

datmtx = [a(1:spts,2)]; % wavelength values

n = ra/spts; % sets range for "for loop" counter

for i = 1:n
    datmtx = [datmtx a(1+(spts*(i-1)):(spts*i),3)];
end
```


Linearization: Performs the Beer-Lambert linearization using the sample and reference matrix.

```
%addref.m

function newmtrx=addref(pulpmtrx,refmtrx)

%pulpmtrx=original pulp spectra matrix
%refmtrx=reorganized reference matrix of same size as pulpmtrx
%newmtrx=new pulp spectra divided through by reference

[r,c] = size(pulpmtrx); % r = # rows of rcdmtrx, c = # col's of rcdmtrx

newmtrx = [pulpmtrx(:,1)]; % column of wavelength values

for n = 2:c
    newmtrx = [newmtrx log10(refmtrx(:,n)./pulpmtrx(:,n))];
end
```

DCT: Performs DCT low pass filtering on spectra.

```
%dctlpf.m

function xfil = dctlpf(x,l)

%x=matrix or column vector to dct lowpass filter
%l=length of filter(i.e. number of poits to keep in dct domain)

y=dct(x);
y(1+1:end,:)=0;
xfil=idct(y);
```

R²: Computes R² values for calibration and prediction curves.

```
% rsqd.m

function rsquared = rsqd(yobs,ypred)

r = yobs - ypred;
sse = norm(r).^2;
sst = norm(yobs - mean(yobs)).^2;
rsquared = 1 - (sse/sst);
```

Disturbance: Adds random offset and slope to spectra.

```
% adddisturb.m

function avgwdist = adddisturb(avgmtrx,m,b,wvspt,wvept)

% avgmtrx = matrix generated by avgtempscan.m
% m = slope disturbance (-m to +m)
% b = offset disturbance (-b to +b)
% wvspt = wavelength start point
% wvept = wavelength end point

% avgwdist = matrix of average scan at each temp and average scan at
each temp
% plus disturbance (i.e., slope and offset)

[r,c] = size(avgmtrx);
lsm = wvept - wvspt;

% lambda shift multiplier
% LS = lambda shift

for i = 1:c-1
    LS = wvspt + lsm*rand(1);
    distmtrx(:,i) = avgmtrx(:,i+1) + (m*2*(rand(1)-.5))*(avgmtrx(:,1)-LS)
+ b*2*(rand(1)-.5));
end

avgwdist = [avgmtrx distmtrx];
```